# Tau isoform–specific stabilization of intermediate states during microtubule assembly and disassembly

Received for publication, May 1, 2019, and in revised form, June 24, 2019 Published, Papers in Press, July 2, 2019, DOI 10.1074/jbc.RA119.009124

**Rebecca L. Best, Nichole E. LaPointe, Jiahao Liang[1], Kevin Ruan, Madeleine F. Shade, Leslie Wilson, and Stuart C. Feinstein[2]**

*From the Neuroscience Research Institute and Department of Molecular, Cellular, and Developmental Biology, University of California Santa Barbara, Santa Barbara, California 93106*

Edited by Enrique M. De La Cruz

**The microtubule (MT)-associated protein tau regulates the critical growing and shortening behaviors of MTs, and its normal activity is essential for neuronal development and maintenance. Accordingly, aberrant tau action is tightly associated with Alzheimer's disease and is genetically linked to several additional neurodegenerative diseases known as tauopathies. Although tau is known to promote net MT growth and stability, the precise mechanistic details governing its regulation of MT dynamics remain unclear. Here, we have used the slowly-hydrolyzable GTP analog, guanylyl-($\alpha$,$\beta$)-methylene-diphosphonate (GMPCPP), to examine the structural effects of tau at MT ends that may otherwise be too transient to observe. The addition of both four-repeat (4R) and three-repeat (3R) tau isoforms to pre-formed GMPCPP MTs resulted in the formation of extended, multiprotofilament-wide projections at MT ends. Furthermore, at temperatures too low for assembly of *bona fide* MTs, both tau isoforms promoted the formation of long spiral ribbons from GMPCPP tubulin heterodimers. In addition, GMPCPP MTs undergoing cold-induced disassembly in the presence of 4R tau (and to a much lesser extent 3R tau) also formed spirals. Finally, three pathological tau mutations known to cause neurodegeneration and dementia were differentially compromised in their abilities to stabilize MT disassembly intermediates. Taken together, we propose that tau promotes the formation/stabilization of intermediate states in MT assembly and disassembly by promoting both longitudinal and lateral tubulin–tubulin contacts. We hypothesize that these activities represent fundamental aspects of tau action that normally occur at the GTP-rich ends of GTP/GDP MTs and that may be compromised in neurodegeneration-causing tau variants.**

Tau is a microtubule-associated protein (MAP)[3] found primarily in neuronal axons and cell bodies. Under normal circumstances, tau is necessary for the establishment of neuronal cell polarity, the maintenance of neuronal cell morphology, and various microtubule-dependent functions such as axonal transport (1–7). Interestingly, although tau knockout mice exhibited a rather modest phenotype (8), tau/MAP1B double-knockout mice exhibited a much stronger phenotype than either individual knockout, demonstrating synergistic and necessary action by both MAPs (9). Additionally, aberrant tau biochemistry has long been correlated with Alzheimer's disease and related dementias, known collectively as tauopathies. Specifically, biochemically altered tau is the primary component of neurofibrillary tangles, one of the two hallmark pathologies of Alzheimer's disease. Furthermore, human genetic analyses have demonstrated that both structural and regulatory errors in tau expression can cause neurodegeneration and dementia in frontotemporal dementia with parkinsonism-17 (FTDP-17), progressive supranuclear palsy, and a number of other tauopathies (10–12). Importantly, the molecular mechanism(s) by which aberrant tau structure–function or regulation results in disease pathogenesis remain unknown, although good evidence supporting both loss– of–function and gain– of–function mechanisms has been presented (12–15). Among the proposed mechanisms underlying pathological tau action is altered tau–microtubule interactions, ultimately leading to microtubule destabilization and tau self-aggregation into neurofibrillary tangles (11, 12). Indeed, the vast majority of known pathological mutations in the tau gene leads to reduced tau affinity for MTs (16–19), reduced ability to regulate MT dynamics (17, 18, 20), and increased propensity of tau aggregation (21, 22).

MTs are dynamic cytoskeletal polymers that are essential for many cellular processes, including cell division, maintenance of cellular shape, intracellular transport, and cell signaling (26–29). The best understood aspect of tau action is to regulate MT dynamics, which are critical in order for MTs to perform their essential functions. The adult human central nervous system expresses six different isoforms of tau, generated by alternative splicing of exons 2, 3, and 10 of the *mapt* gene (30). The pres-

This work was supported, in whole or in part, by UCSB Academic Senate Research Grant 2017–2018 (to S.C.F.) and National Science Foundation Grant 1650114 (to R.L.B.). The authors declare that they have no conflicts of interest with the contents of this article.

This article contents Figs. S1–S3, Tables S1–S7, and supporting Information.

[1] Present address: Dept. of Pharmaceutical Chemistry, University of California San Francisco, 1700 4th St., San Francisco, CA 94158.

[2] To whom correspondence should be addressed: Neuroscience Research Institute, Bldg. 571, Rm. 6129, University of California Santa Barbara, Santa Barbara, CA 93106. Tel.: 805-893-2659; Fax: 805-893-2659; E-mail: feinstei@lifesci.ucsb.edu.

[3] The abbreviations used are: MAP, microtubule-associated protein; MT, microtubule; FTDP-17, fronto-temporal dementia with parkinsonism linked to chromosome 17; 3R, 3-repeat tau; 4R, 4-repeat tau; GLM, generalized linear model; OH, ordered heterogeneity; GMPCPP, guanylyl-($\alpha$,$\beta$)-methylene-diphosphonate; TEM, transmission EM; ANOVA, analysis of variance.

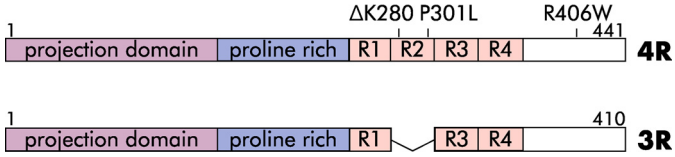


**Figure 1. Schematic of 4R (*top*) and 3R (*bottom*) tau with major features labeled, including the MT-binding repeats (*R1–R4*).** Additional labels indicate pathological (ΔK280, P301L, R406W) mutations.

ence or absence of exon 10 in adults leads to the approximately equal expression of tau proteins possessing three or four adjacent, 31-amino acid–long, imperfect MT-binding repeats (designated as 3R or 4R tau, respectively, see Fig. 1). Notably, mutations in the *mapt* gene that disrupt the normal 3R/4R tau isoform ratio, leading to the overproduction of wildtype (WT) 4R tau, cause dementia (31, 32). Mechanistically, 3R and 4R tau regulate MT dynamics by (i) lowering the critical concentration of tubulin dimers required for MT assembly, (ii) moderately increasing MT growth rates, (iii) increasing the amount of time MTs spend in an attenuated or static state, and (iv) suppressing the frequency of MT catastrophes (a switch from a growing or attenuated state to a shortening state) (13, 26, 29, 34). Importantly, 4R tau suppresses MT shortening rates and shortening lengths per event much more effectively than does 3R tau (1, 13, 35, 36). Despite these insights, the underlying mechanism(s) by which tau binding to MTs and tubulin heterodimers mediates its regulation of MT dynamic instability remains poorly understood.

Multiple tau-binding sites upon MTs have been reported, including sites along the outer MT surface (37–40), at the longitudinal interface between heterodimers (41), and within the MT lumen (interior) (42, 43). Importantly, kinetic analyses *in vitro* (44) and in cells (45) indicate that tau has at least two modes of binding to MTs, one that is transient and readily exchangeable with tau in solution and another that is relatively nonexchangeable. The nonexchangeable binding site appears to be accessible only when tau is present during MT assembly and not when tau is added to pre-assembled MTs (44). The notion of a strong association between tau and MTs contrasts with recent studies indicating that tau's association with MTs is highly dynamic (46–49). These data are all compatible with a model in which the dynamic tau population corresponds to the readily dissociable binding mode on the outside of the MT, while the second very stable binding mode corresponds to the tau-binding site within the lumen of the MT as described by Kar *et al.* (42).

Tau binding to MTs reaches saturation at a molar ratio on the order of 1 tau per ~5–10 tubulin dimers (26, 50, 51), implying a high abundance of binding sites along the length of an MT. However, the abundance of these sites could obscure a much lower abundance of higher-affinity tau-binding sites at MT ends, where growing and shortening events occur. Indeed, this is the case for the MT-binding drug vinblastine (52–55). Tau also binds to free tubulin heterodimers and is capable of binding multiple heterodimers simultaneously via multiple motifs within the MT-binding repeats as well as sequences in the adjacent "pseudorepeat" R′ (38, 56, 57). These regions of tau can also interact with multiple sites on free tubulin heterodimers, including, but not limited to, the disordered, negatively-charged C-terminal "tails" of $\alpha$- and $\beta$-tubulin (56, 57), which are also important for tau binding on the outer MT surface (38, 39, 58).

Nucleation, the rate-limiting step in MT assembly, is a complex process that culminates in the formation of the smallest energetically favorable tubulin oligomer necessary to promote assembly (59). Although the identity of this intermediate has remained elusive, a number of transient intermediate structures have been reported, including rings, twisted ribbons, and sheets (40, 60–68). During nucleation, GTP-bound tubulin heterodimers first associate head–to–tail via longitudinal contacts to form protofilaments, which then associate via lateral contacts to form an MT (59, 69). Protofilaments are curved in solution but are straight within the context of the MT lattice, constrained by lateral contacts with neighboring protofilaments (68, 70–73).

Dynamic MT ends can switch stochastically between phases of assembly and disassembly. At the heart of this "dynamic instability" is the hydrolysis of GTP by $\beta$-tubulin, which occurs at the longitudinal interface between two heterodimers following incorporation into the MT lattice and is thought to be accompanied by conformational changes that introduce additional lattice strain (72, 73). MTs have been proposed to possess a stabilizing "GTP" or "GDP-Pi" cap at their plus-ends composed of tubulin heterodimers that have not yet undergone conversion to GDP. This cap serves to promote further MT elongation and prevent "catastrophe," a switch to a rapidly-shortening state in which lateral contacts between protofilaments are lost and protofilaments peel outward from the body of the MT. While early models attributed the stabilizing effect of the GTP cap and assembly competency of GTP tubulin to an inherent difference in protofilament curvature between the GTP and GDP state (with GTP possessing a straight conformation), more recent work indicates that whereas GTP tubulin is straighter than GDP tubulin, it is also curved, arguing that straightening occurs as MT-specific lateral contacts are established (73, 74). Thus, rather than protofilament curvature, the most recent picture of the conformational changes that accompany GTP hydrolysis includes compaction of the interface between longitudinally-associated heterodimers and rotation of $\alpha$-tubulin into a more bent structure (73, 75).

In an attempt to better understand how tau mechanistically regulates MT assembly and dynamic instability, we examined the action of tau at MT ends through experiments with the slowly-hydrolysable GTP analog GMPCPP (76). MTs assembled with GMPCPP tubulin are widely believed to model the GTP-rich end of a normal (*i.e.* GTP/GDP)-growing MT (70, 71, 73, 74, 76).

This idea is supported by the fact that GTP and GMPCPP tubulin both maintain similar lateral contacts (73). Additionally, approximately equal MT elongation rates are observed in the presence of GMPCPP and GTP (76). Furthermore, despite GMPCPP tubulin's enhanced nucleation abilities, early *in vitro* MT assembly experiments comparing the two nucleotides show that the same intermediate structures were produced in the early phases of MT nucleation, albeit in much larger quantities in GMPCPP-containing samples (62). We reasoned that

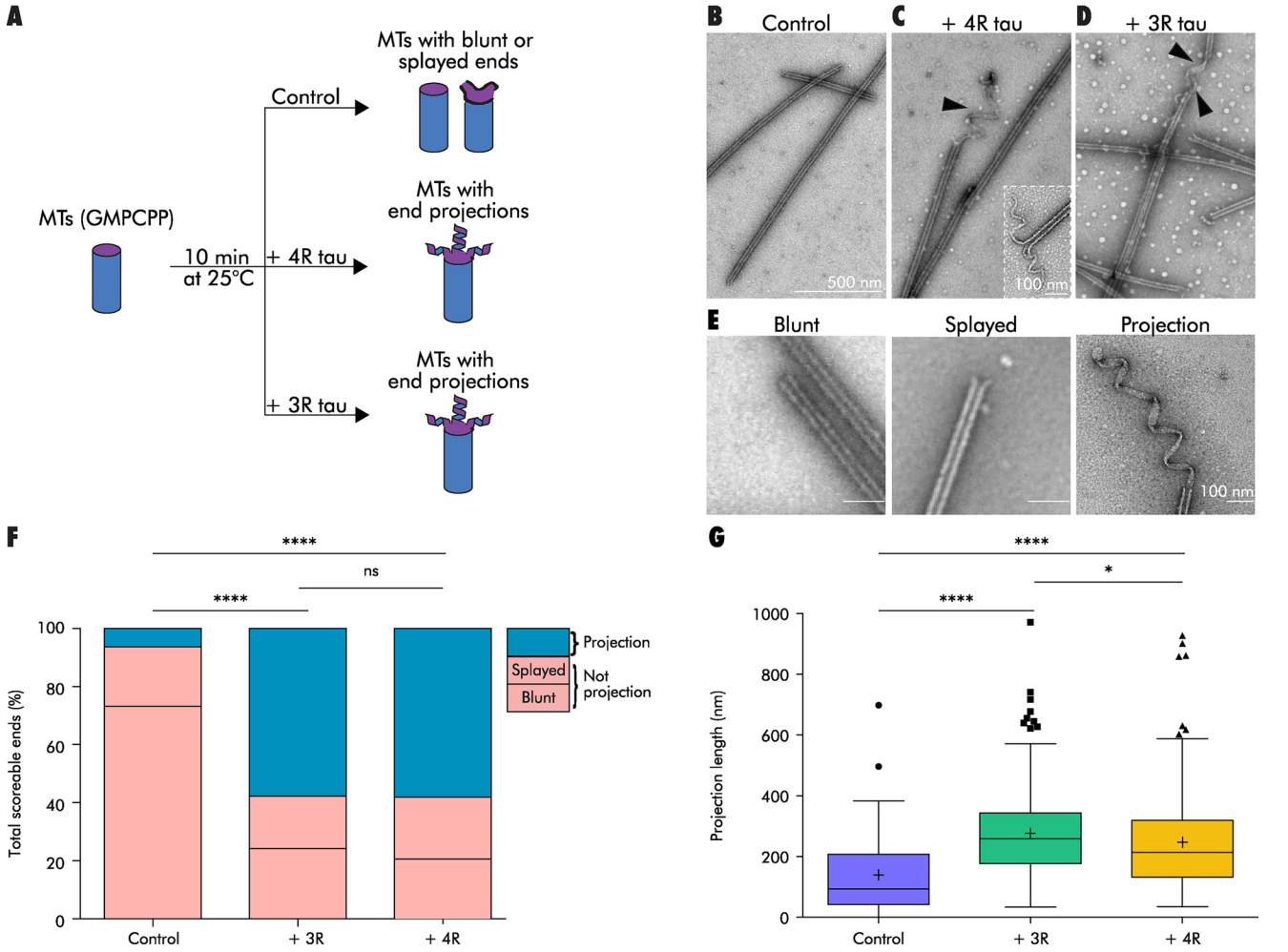


**Figure 2. Tau stabilizes projections at the ends of pre-assembled GMPCPP microtubules.** *A,* schematic of a GMPCPP MT decoration assay. *B,* GMPCPP MTs in the absence of tau possess blunt or splayed ends. *C* and *D,* GMPCPP MTs decorated with 4R tau or 3R tau, respectively, develop spiral, ribbon-like projections at microtubule ends (*black arrowheads*). *Inset:* high magnification image of an end projection. *E,* scoring guide for MT ends. *F* and *G,* projection frequency (*F*) and length (*G*) of GMPCPP MTs (0.5 $\mu$M) decorated with buffer or tau (4R or 3R, 1:5 tau/tubulin molar ratio). *Bars* show total counts summed across all experiments. Tukey's boxplot, *horizontal line* at the median, *plus sign* at the mean. Outliers shown as individual points. *, $p < 0.05$; ****, $p < 0.0001$, *ns*, not significant. See also Table S1.

the use of GMPCPP, with its enhanced nucleation ability and overall higher stability, might enable us to observe structural intermediates that would ordinarily be too transient to detect.

Here, we show that pre-assembled GMPCPP MTs develop extended projections composed of multiple aligned protofilaments upon the addition of tau. Furthermore, at temperatures too low for MT assembly, GMPCPP tubulin heterodimers co-incubated with tau form numerous long spirals reminiscent of the end projections observed at higher temperatures on pre-formed MTs. Next, GMPCPP MTs undergoing disassembly in the presence of 4R tau (and to a lesser extent 3R tau) also form spirals. Finally, we show that three tau mutations that cause neurodegeneration and dementia are compromised in their ability to stabilize MT disassembly intermediates. Taken together, we propose that tau acts to promote both longitudinal and lateral contacts to stabilize intermediate states that can be reached via both assembly and disassembly and that some of these abilities may be compromised in pathological tau. We hypothesize that these activities represent fundamental aspects of tau action that normally occur at the GTP-rich ends of GTP/GDP MTs.

## Results

Given tau's potent regulation of MT dynamic instability, we focused our attention upon tau action at MT ends, where tau's regulatory effects upon dynamics must ultimately be put into action.

### *Tau promotes the stabilization of tubulin projections at the ends of pre-assembled GMPCPP microtubules*

Pre-assembled GMPCPP MTs (at a final concentration of 0.5 $\mu$M tubulin) were incubated in buffer, plus or minus tau at a molar ratio of 1:5 tau/tubulin, for 10 min at 25 °C in a "decoration" assay (Fig. 2*A*). We then examined MT end morphologies using transmission EM (TEM).

In the absence of tau, nearly all of the GMPCPP MTs possessed normal blunt or slightly splayed end morphologies (Fig. 2, *B* and *E*), whereas the addition of 4R or 3R tau resulted in coiled projections at many ends (Fig. 2, *C–E*). The tau effect was rapid, specific, and observed across multiple independent tubulin and tau preparations (this is true for all experiments

reported in this study). Specifically, projections appeared within ~1 min of tau addition and were not observed when pre-assembled MTs were decorated with the MT-stabilizing drug taxol, the MT end-binding protein EB1, or the non-MT–interacting proteins with overall negative (BSA) or positive (histone) charges (Fig. S1*A*).

To quantitatively assess these data, we developed a scoring system for the different MT end morphologies (Fig. 2*E*). "Blunt" and "splayed" describe normal MT end morphologies lacking "projections," with a splayed end having a slight gap between terminal protofilaments. Projection describes MT ends possessing either one projection >25 nm in length (one MT diameter) or at least three projections (with no length minimum). MT ends not fitting into any of the above three categories were extremely rare (~2%) and were therefore excluded from the analysis.

As seen in Fig. 2*F* and Table S1, projection frequencies significantly differed between the no-tau control samples and the tau-decorated MTs (generalized linear model (GLM), $p < 0.0001$). Control MTs exhibited almost exclusively blunt and splayed ends, with only 6.3% of ends possessing projections. In contrast, MTs decorated with either 4R tau or 3R tau had greatly increased projection frequencies relative to the no-tau control (57.7 and 57.8%, respectively; $p < 0.0001$ for both comparisons), whereas the two tau isoforms were not different from one another. Interestingly, these end projections appeared to be derived primarily from blunt-ended MTs as opposed to those with a splayed morphology (Fig. 2*F*).

Finally, MT length distributions measured before and after decoration with tau revealed no detectable change in MT length (excluding projection length) over the 10-min incubation at 25 °C (Fig. S1*B*).

### *Are tubulin projections at MT ends the result of tau-mediated effects during MT assembly, disassembly, or both?*

Projections at MT ends could result from tau-promoted growth via addition of soluble tubulin heterodimers onto existing MT ends, perhaps analogous to the curved protofilament sheets observed at fast-growing MT ends (68). However, because the final step in our GMPCPP MT preparation is centrifugation and resuspension in tubulin-free buffer (see under "Experimental procedures"), only minimal quantities of free tubulin heterodimers are expected to be present in these preparations. However, GMPCPP tubulin has an estimated critical concentration of only 20 nM for nucleated assembly onto pre-existing MTs (76), and the critical concentration could be even lower in the presence of tau. Therefore, we hypothesized that small amounts of free tubulin subunits present in the GMPCPP MT preparation (carried over after centrifugation and/or arising during the storage process) might be sufficient to support some small amount of tau-mediated assembly at MT ends. Alternatively, if the projections were generated during MT disassembly events, the simplest model would be that the projections represent a normally short-lived disassembly intermediate that is stabilized by tau, perhaps analogous to the protofilament peels observed at the ends of disassembling MTs (70, 77–80).

#### *Tau-induced projections form during MT assembly events*

To begin assessing whether the projections in the decoration assays (Fig. 2) were the result of tau action during MT assembly, disassembly, or both, we exploited a differential activity of 4R and 3R tau that we and others have described *in vitro* and in cultured cells; although both 4R and 3R tau promote MT growth events to a similar extent, 4R tau suppresses MT shortening events much more effectively than does 3R tau (1, 13, 28, 35, 36, 81). Therefore, if the MT end projections were formed by tau action during MT assembly, 4R and 3R tau would be predicted to exhibit comparable projection formation abilities. Alternatively, if the projections were generated by tau action during MT disassembly, 4R tau would be predicted to exhibit increased projection frequency and/or longer projection lengths than those exhibited by 3R tau.

*3R tau and 4R tau generate similar projections in MT decoration assays, supporting tau-mediated formation of end projections during MT assembly events*—The decoration assay presented in Fig. 2, in addition to revealing the existence of MT end projections in the presence of 4R and 3R tau, also addresses the question of whether or not projections can form during MT assembly events. For example, at a 1:5 tau/tubulin molar ratio (where the MT lattice is saturated with tau and where 3R tau promotes MT growth comparably to 4R tau (13, 36)), we found that the distribution of MT end morphologies was essentially identical with both tau isoforms (Fig. 2*F* and Table S1). Furthermore, projections were similar lengths with both isoforms. 3R-decorated MTs had projections that were slightly longer, with a mean length of 275 ± 8.9 nm compared with 4R-decorated MTs with a mean length of 245 ± 9.3 nm. Both were significantly longer than the relatively rare projections observed in the no-tau controls (mean length 138 ± 13 nm, $p < 0.0001$ for both comparisons; Fig. 2*G* and Table S1). The small (30 nm) length difference between 3R- and 4R tau-promoted projections was statistically significant ($p = 0.017$). Nonetheless, the similar lengths and nearly identical abundance of 4R- and 3R-induced end projections support the notion that the projections are the result of tau-mediated stabilization of an assembly event. The simplest interpretation is that low levels of free tubulin subunits present in the assay mixtures were sufficient to support projection assembly.

We next reasoned that although sufficient for some amount of projection assembly, the low level of free tubulin in the decoration assay could be a limiting factor. Therefore, as an additional assessment of the assembly origin model for projections, we performed decoration assays in which we supplemented the system with an additional 0.5 μM free GMPCPP tubulin. In the presence of the additional tubulin, we observed increases in both projection frequency and projection length in tau-containing samples. Specifically, projection frequency for 4R and 3R tau increased by 23 and 11%, respectively, whereas the projection length increased by 43 and 30%, respectively.

Taken together, these data indicate that tau-promoted tubulin assembly activity contributes to the generation of MT end projections.

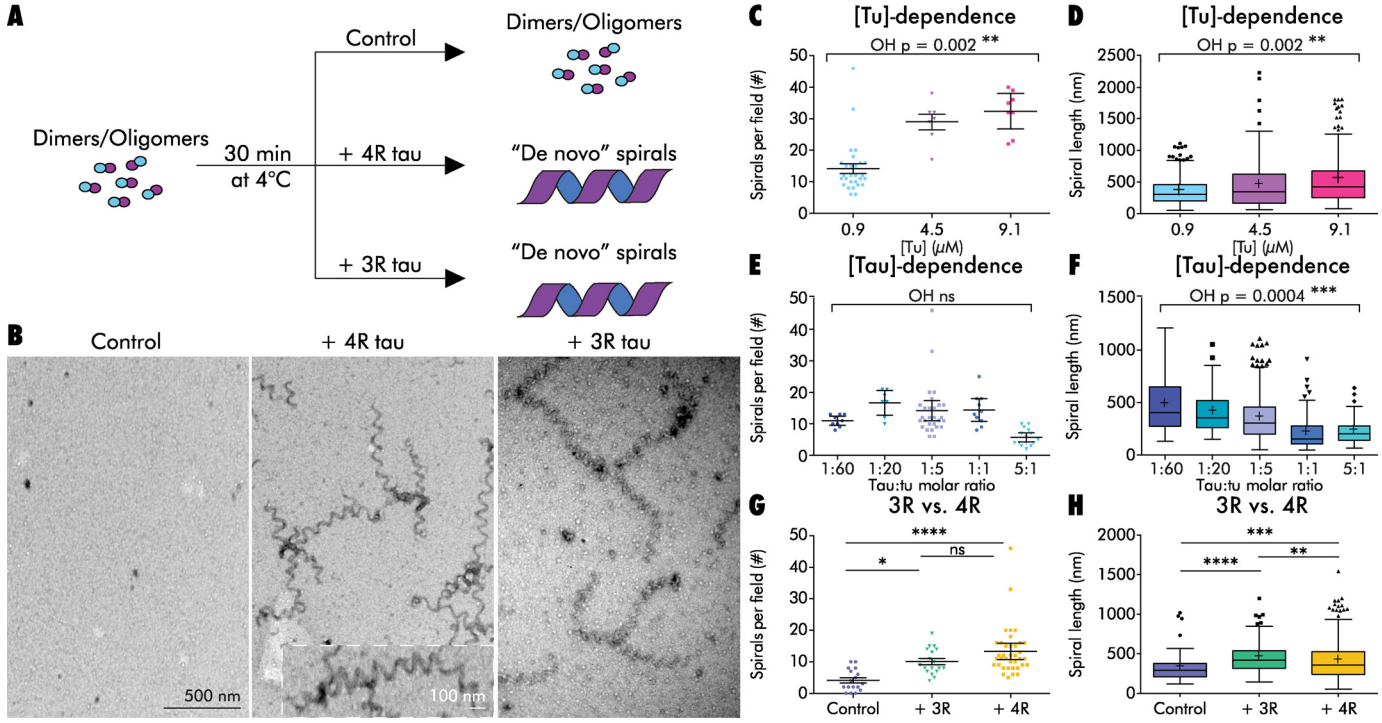


**Figure 3. Tau stabilizes a GMPCPP tubulin spiral structure under nonassembly-promoting conditions.** *A,* schematic of a GMPCPP tubulin *de novo* spiral formation experiment. *B, left*: GMPCPP tubulin dimers (0.9 μM) in the absence of tau only rarely form spirals. *Center* and *right*: in the presence of 4R tau and 3R tau, respectively (1:5 tau/tubulin molar ratio), GMPCPP tubulin dimers assemble into plentiful spirals. *Inset* shows a higher magnification image of a *de novo* spiral. *C* and *D,* effects of tubulin concentration on *de novo* spiral abundance (*C*) and length (*D*) with 4R tau at a constant 1:5 tau/tubulin molar ratio. *E* and *F,* effects of 4R tau concentration on *de novo* spiral abundance (*E*) and length (*F*) at a constant tubulin concentration of 0.9 μM. *G* and *H, de novo* spiral abundance (*G*) and lengths (*H*) with 3R and 4R tau (1:5 tau/tubulin molar ratio). *Graphs* (*D, F,* and *H*) are Tukey's boxplots. *Graphs* (*C, E,* and *G*) show mean and 95% confidence interval (*CI*); each data point represents a randomly chosen field at ×30,000 magnification. ****, $p < 0.0001$; ***, $p < 0.001$; **, $p < 0.01$; *, $p < 0.05$, *ns*, not significant. See also Tables S2–S4.

*In the absence of MT assembly, tau promotes formation of GMPCPP tubulin "spirals"*—Interestingly, the decoration experiment presented in Fig. 2 did not result in a measurable change in MT length (Fig. S1*B*). Therefore, we next asked whether tau can promote the assembly of any alternative tubulin structures in the absence of pre-formed MTs, such as the rings, "twisted ribbons," and/or sheets observed at the earliest time points of MT assembly reactions under various conditions (40, 63, 66, 82–84). It is especially notable that spirals observed with GMPCPP tubulin and high concentrations of $Mg^{2+}$ can directly convert into MTs and have been proposed to correspond to sheet-like intermediates observed at growing MT ends (84).

To prevent assembly of complete MTs and therefore increase the likelihood of observing pre-MT structures, we performed our experiments at 4 °C. We incubated 0.9 μM GMPCPP tubulin heterodimers for 30 min at 4 °C in the presence or absence of 4R or 3R tau (Fig. 3*A*). Under these conditions, both 4R tau and 3R tau promoted the assembly of long GMPCPP tubulin spirals (Fig. 3*B*), which we term "*de novo*" spirals to emphasize that the starting material was unpolymerized tubulin dimers rather than pre-assembled MTs. No tau-containing control samples possessed far fewer and significantly shorter spirals (Fig. 3, *B, G,* and *H*). The fact that spirals were observed even in the absence of tau suggests that these GMPCPP tubulin spirals, like those observed by Wang *et al.* (84, using different conditions), represent a normal intermediate in GMPCPP tubulin assembly.

Width measurements from TEM images indicated that *de novo* spirals were 25.2 ± 0.9 nm, suggesting that our *de novo* spirals were composed of an average of ~6 protofilaments. Both spiral number (ordered heterogeneity, OH $p = 0.002$) and spiral length (OH $p = 0.002$) were positively correlated with tubulin concentration (holding the tau/tubulin ratio constant; Fig. 3, *C* and *D*, and Table S2). In contrast, spiral length (OH $p = 0.0004$; Fig. 3*F* and Table S3) but not spiral number (Fig. 3*E* and Table S3) negatively correlated with increasing tau/tubulin molar ratios. One simple interpretation compatible with all of these data is that an increased number of tau molecules results in an increased number of spiral nucleation events, ultimately resulting in an increase in spiral abundance and a decrease in average spiral length as tubulin subunits become limiting. This would be consistent with tau lowering the critical concentration for spiral formation. In contrast, the trend toward increased spiral abundance at higher tau/tubulin molar ratios did not reach statistical significance (Fig. 3*E* and Table S3).

Next, we asked whether both 3R and 4R tau isoforms promote *de novo* spiral assembly to the same extent. We incubated 0.9 μM GMPCPP tubulin alone or with 3R or 4R tau (1:5 tau/tubulin molar ratio) and then quantified spiral abundance and length. The three conditions differed significantly in both the numbers (ANOVA $p < 0.0001$) and lengths (Welch's ANOVA $p < 0.0001$) of *de novo* spirals. We found comparable numbers of *de novo* spirals in the presence of 3R tau and 4R tau (Table S4). Both tau isoforms assembled more spirals than controls ($p = 0.011$ *versus* 3R tau and $p < 0.0001$ *versus* 4R; Fig. 3*G*).

Spirals were also longer in the presence of either tau isoform than in the no-tau control ($p < 0.0001$ *versus* 3R tau and $p = 0.0008$ *versus* 4R tau). 3R tau produced the longest spirals, with a mean length of 450 ± 14 nm, compared with 402 ± 11 nm with 4R tau, and 319 ± 20 nm in controls (Fig. 3*H* and Table S4). The length difference between 3R tau and 4R tau was statistically significant ($p = 0.008$). This observation is reminiscent of the longer projection lengths observed with 3R tau relative to 4R tau in the decoration assay (Fig. 2). Both of these observations would be predicted if 4R tau is a slightly stronger nucleator of spiral and MT formation (*i.e.* given limited free tubulin subunits, more nucleation events would result in shorter average lengths). Consistent with our earlier observations, a large increase in the tau concentration (to 5:1 tau/tubulin molar ratio) resulted in decreased mean spiral lengths for both 3R and 4R tau samples, giving spirals with mean lengths of 363 ± 14 and 364 ± 8.5 nm, respectively. These data are consistent with the comparable assembly-promoting activities of 3R and 4R tau reported in the literature and support the notion that spirals represent a tau-stabilized intermediate in MT assembly.

*Under MT assembly conditions, incubation of tau with GMPCPP tubulin supports the model that tau prolongs an intermediate assembly state*—Tau's ability to promote the assembly of *de novo* spirals under non-MT assembly conditions coupled with the assembly of a lesser number of spirals even in the no-tau controls led us to hypothesize that the spirals represent a normal intermediate in GMPCPP MT assembly and a fundamental component of tau action in MT assembly. Wang *et al.* (84) demonstrated that GMPCPP tubulin spirals formed at 4 °C and high $Mg^{2+}$ concentrations could undergo a temperature-dependent conversion into MTs (without a depolymerization step), leading the authors to hypothesize a connection between their spirals and the sheet-like intermediates sometimes observed at the ends of fast-growing GTP MTs (84). The Wang *et al.* (84) transition from spirals to MTs occurred around 25 °C, the critical temperature for GTP tubulin assembly (84). To determine whether our tau-induced *de novo* spirals could also transition to *bona fide* MTs, we prepared *de novo* spirals as above (0.9 μM GMPCPP tubulin, 1:5 4R tau/tubulin molar ratio, 30 min at 4 °C), then warmed the solution to 34 °C, and examined the samples by TEM. Control reactions lacking tau contained abundant MTs with normal morphology. In contrast, we found few morphologically normal MTs in 4R tau-containing samples and instead observed tangled clumps of MTs, spirals, and ribbon-like sheets (data not shown).

We reasoned that our conditions might promote the formation of very long spirals that become highly tangled, thereby interfering with the temperature-induced conversion into MTs. To provide conditions in the tau samples that might be more conducive to complete MT assembly, we eliminated the incubation at 4 °C. Additionally, we increased the tubulin concentration to promote more nucleation events. Therefore, we repeated the tau plus tubulin co-assembly experiment at 6.6 μM tubulin (1:5 tau/tubulin). Reaction components were mixed together on ice and then immediately warmed to 34 °C. We took TEM samples as soon as possible (~ 5 min) after tau addition (in warm buffer, simultaneous with the temperature change) and then after 30 min and 24 h at 34 °C. Before the temperature increase, TEM revealed no visible structures (data not shown). In the absence of tau, MTs were observed at 5 min and greatly increased in number by 30 min (Fig. 4*B*). At these time points, the no-tau controls showed occasional spiral and ribbon-like structures, both free and at MT ends (Fig. 4*B*). By 24 h, most of these control MTs had normal end morphologies without projections. In contrast, non-MT structures were both much more common and longer at all time points in samples containing 4R tau. Spirals, but not MTs, were observed at 5 min (Fig. 4*B*). By 30 min, some rare MTs with long end projections were also present, although in tangled masses of spirals, MTs,

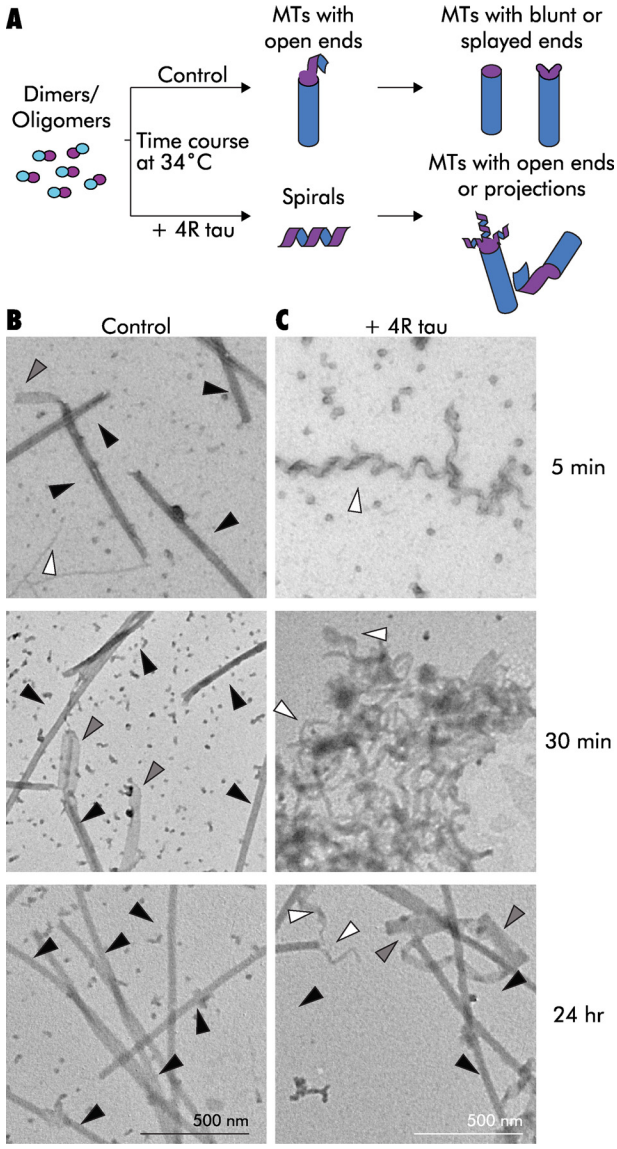


**Figure 4. TEM time course of GMPCPP tubulin assembly at 34 °C suggests that tau prolongs an intermediate structural state.** *A,* schematic of a warm co-assembly experiment. *B,* assembly time course of 6.6 μM GMPCPP tubulin in the absence of tau. Note the presence of MTs (*black arrowheads*), spirals/projections (*white arrowheads*), and ribbon/sheet structures (*gray arrowheads*) after only 5 min. By 30 min, more MTs and sheet structures that may be unfolded MTs have formed. By 24 h, there are many MTs with normal morphology. *C,* assembly time course in the presence of 4R tau (1:5 tau/tubulin molar ratio). Note the lack of MTs at the earliest time point. By 30 min, MTs are still scarce and large, and tangled clumps of spirals are visible. After 24 h, some MTs are present, although tangled clumps and ribbons are still plentiful, especially in proximity to MT ends.

and sheet- or ribbon-like structures (Fig. 4*B*). Width measurements suggested that some of these structures might represent unfolded, or not-yet-folded, MTs (average ~75 ± 9.6 nm, which is the predicted circumference of MT). After 24 h, the 4R tau-containing sample showed more MTs than the 30-min sample, but many had long end projections, and tangled masses were still present. Parallel experiments demonstrated that 3R tau also stabilized spirals and produced similar tangled masses as well as some normal MTs (data not shown). Importantly, parallel co-assembly experiments of GTP tubulin both with and without 4R tau yielded morphologically normal MTs (1:5 tau/tubulin molar ratio; Fig. S2). Substitution of the MT-stabilizing drug taxol for tau also led to MTs lacking projections. Taken together, the data support the notion that the spirals represent a prolonged view of a normally transient intermediate, assembled and stabilized as a result of normal tau activity.

### *Tau stabilizes tubulin spirals during GMPCPP microtubule disassembly*

The results described above indicate that tau stabilizes an intermediate structure during the process of MT assembly. Next, we asked whether or not 4R tau, as a more potent stabilizer against MT shortening relative to 3R tau, more effectively stabilizes any MT disassembly intermediates compared with 3R tau. We returned to the use of pre-assembled GMPCPP MTs and pushed them toward cold temperature-induced disassembly in the presence or absence of 4R or 3R tau. If 4R is more effective than 3R tau, it should stabilize an MT disassembly intermediate that is more abundant and/or longer than similar non-MT structures observed in the presence of 3R tau or the no-tau controls.

We induced disassembly by diluting pre-assembled GMPCPP MTs into ice-cold buffer alone or in buffer containing tau (final tubulin ~0.5 $\mu$M, final molar ratio 1:5 tau/tubulin) and examined the structures present after 10 min by TEM (Fig. 5*A*). In the absence of tau, diluted MTs disassembled almost completely, containing only rare spirals (Fig. 5*B*). We refer to these as "disassembly" spirals to emphasize their origin from depolymerizing MTs. In contrast, MTs disassembled in the presence of 4R tau resulted in the presence of many more disassembly spirals than either 3R or control (Welch's ANOVA $p < 0.0001$; Fig. 5, *B* and *C*). Specifically, 4R tau exhibited an average of 19 ± 1.4 spirals per field, compared with 3.7 ± 0.7 and 2.0 ± 0.3 for 3R tau ($p < 0.0001$) and the no-tau controls ($p < 0.0001$), respectively (Fig. 5*C* and Table S5). We also observed significant differences in spiral lengths (Welch's ANOVA, $p < 0.0001$). 4R tau-stabilized spirals were significantly longer on average (497 ± 14 nm) than the occasional 3R tau-stabilized spirals (324 ± 16 nm, $p < 0.0001$) or control spirals (296 ± 23, $p < 0.0001$; Fig. 5*D* and Table S5). It is also notable that 3R tau had a comparatively small, although statistically significant, effect in terms of both the spiral abundance and length *versus* the control samples ($p = 0.046$ and $p = 0.014$, respectively). Taken together, all of these data fit well with the well-established observation that 4R has a markedly more potent effect upon MT shortening events than does 3R tau (1, 13). Increasing the tau/tubulin ratio from 1:5 to 10:1 (holding the tubulin concentration constant) had no effect on spiral abundance or length for both 4R and 3R tau (data not shown), indicating that tau isoform-specific differences in disassembly spiral stabilization are intrinsic properties of the proteins themselves.

In all cases measured, disassembly spirals were an average of 18.1 ± 0.4 nm wide, corresponding to ~4 protofilaments wide. Together with the fact that the disassembly spirals were differentially stabilized by 4R tau *versus* 3R tau, this suggests that they may be distinct from *de novo* spirals.

MTs are known to be more resistant to cold-induced disassembly at higher concentrations (85). Therefore, we hypothesized that performing the same disassembly experiment at a higher MT concentration might slow depolymerization and allow us to better observe the transition from MTs to disassembly spirals. We cooled GMPCPP MTs (6.1 $\mu$M) to 4 °C in the presence or absence of 4R tau (1:4 tau/tubulin; Fig. 5, *E* and *F*). We took TEM samples immediately after tau addition (in ice-cold buffer, simultaneous with the temperature change) and then again after 60 min. MT length measurements indicated that MTs disassembled over time to a nearly identical extent in the presence and absence of tau, from 3.1 ± 0.1 to 2.1 ± 0.1 $\mu$m in the no-tau controls (two-sample bootstrap $p < 0.0001$) and from 3.0 ± 0.1 to 2.2 ± 0.1 $\mu$m with 4R tau (two-sample bootstrap $p < 0.0001$; Fig. S3). Importantly, the ends of control MTs showed few projections during disassembly, with an average of 1.3 ± 1.0 projections per field (15% of total MT ends) at the initial time point and 2.8 ± 0.9 projections per field (20% of total MT ends) at the 60-min time point (Fig. 5*G*). In contrast, end projections for MTs incubated with 4R tau drastically increased in frequency over time, from 4.3 ± 0.8 projections per field (22% of total MT ends) initially to 28 ± 9.8 projections per field (94% of total MT ends) after 60 min (Fig. 5*G*). This is consistent with the results from Muller-Reichert *et al.* (70), showing that ~90% of both GDP and GMPCPP MT ends possessed "curved oligomers" upon inducing MT disassembly with high concentrations (24 mM) of $Ca^{2+}$.

MTs disassembled in the presence of 4R tau had an average of 26 more projections per field at 60 min than the no-tau control samples (two-sample Alexander-Govern $p = 0.040$; Fig. 5*G*). The average projection length increased over time for both conditions, although the difference of 4R tau was not statistically significant. The no-tau control projection lengths increased from 69 ± 9.2 to 169 ± 33 nm (difference in confidence intervals, $p = 0.039$), despite the low number of projections observed at each time point ($n = 8$ for 0 min and $n = 12$ for 60 min). Projection lengths in 4R tau-containing samples increased from 194 ± 29 to 255 ± 18 nm, but this difference was not statistically significant (two-sample bootstrap $p = 0.068$; Fig. 5*H*). The lack of statistical significance for the 4R tau samples may due to the high variability in projection lengths exhibited by 0-min 4R tau samples ($n = 25$). Nonetheless, it is important to note that the presence of 4R tau resulted in longer and more numerous projections than the no-tau controls at each time point. These data suggest that 4R tau stabilizes an intermediate structure during MT disassembly, which may contribute to the ability of 4R tau but not 3R tau to stabilize MTs against catastrophe (1, 13, 35, 36).

Taken together, these analyses demonstrate the ability of 4R tau to stabilize an intermediate during MT disassembly.

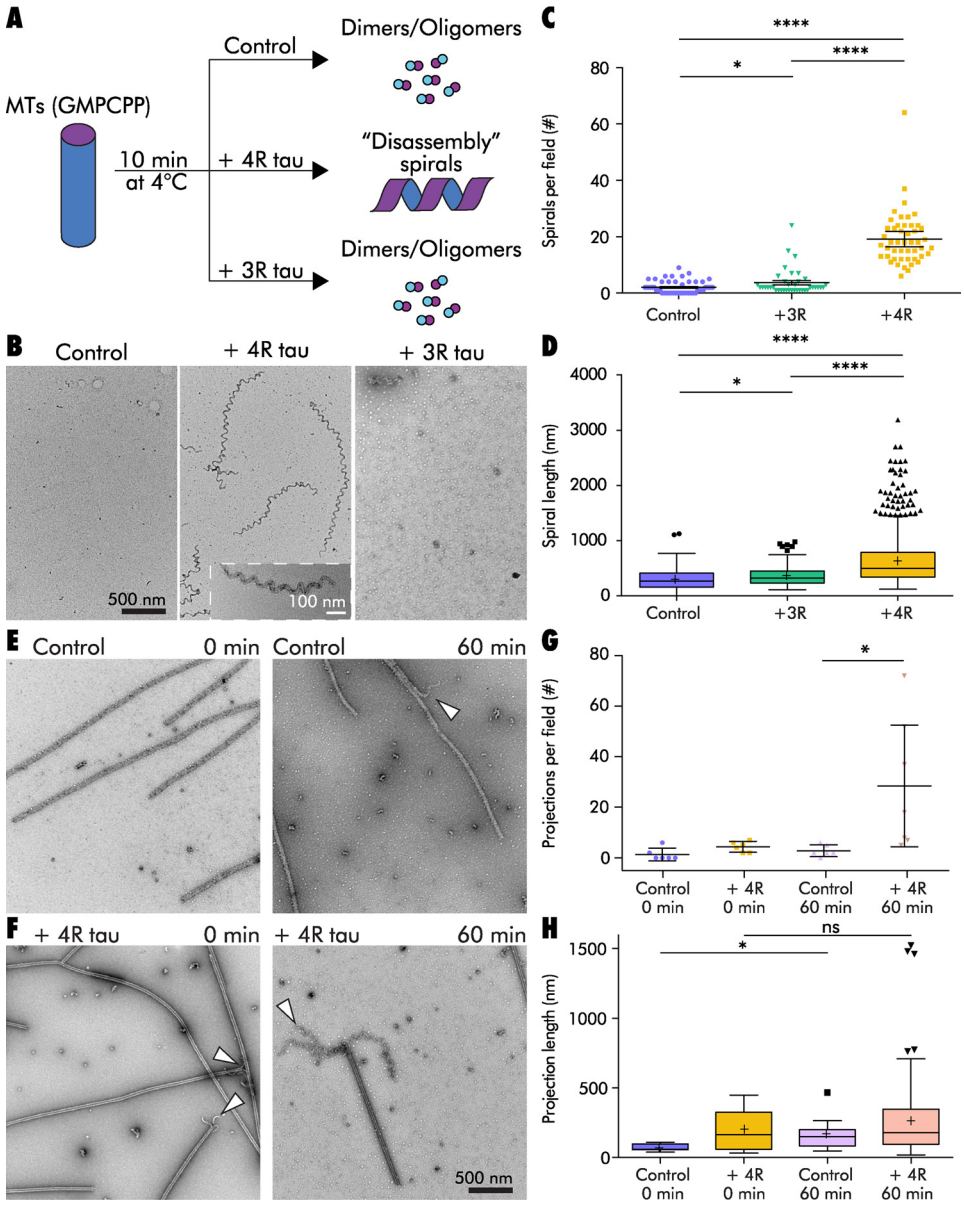


**Figure 5. Tau stabilizes a GMPCPP tubulin spiral structure that is reached through microtubule disassembly.** *A,* schematic of a disassembly spiral experiment. *B,* GMPCPP MTs (0.5 $\mu$M) diluted into ice-cold buffer in the absence of tau (*left*) or in the presence of 3R tau (*right*) disassemble into tubulin dimers and/or oligomers, with the occasional spiral observed. Cold dilution in the presence of 4R tau results in disassembly spirals (*center*). *Inset* shows a higher magnification image of a disassembly spiral. *C* and *D,* disassembly spiral abundance (*C*) and length (*D*) from MTs disassembled in the presence of 3R or 4R tau. *E* and *F,* time course of 6.1 $\mu$M GMPCPP MTs cooled to 4 °C in the absence (*E*) or presence (*F*) of 4R tau (1:4 tau/tubulin molar ratio). Note the presence of projections at MT ends in the presence of tau, even at the earliest time point (*left*), and persistence of MTs in both samples, even after 60 min (*right*). *G* and *H,* projection abundance (*G*) and length (*H*) from *E* and *F*, shown from one representative experiment. ****, $p < 0.0001$; *, $p < 0.05$. *ns*, not significant, $p > 0.05$. See also Table S5.

### *Three FTDP-17 tau mutants are differentially compromised in their ability to stabilize disassembly spirals*

We hypothesized that if the stabilization of intermediate structures in MT assembly and disassembly is a normal physiological tau activity, then it may be compromised by disease-associated mutations in the tau gene. We therefore assessed the effects of three known human tau mutations that cause neurodegeneration, ΔK280, P301L, and R406W, for their abilities to stabilize (i) assembly projections at MT ends and (ii) disassembly spirals. At a structural level, the P301L and ΔK280 mutations map within the MT-binding repeat region, whereas R406W maps downstream of the M- binding repeat region in the C-terminal tail of the protein (Fig. 1). Functionally, P301L and ΔK280 exhibit loss–of–function effects on MT-binding affinity and the ability to regulate MT dynamics (15–20). They also aggregate more readily than WT tau (21, 22). Although R406W also causes disease, it has less marked effects on these parameters (17, 18, 86).

We performed MT decoration experiments at 25 °C at a 10:1 tau/tubulin molar ratio with WT 4R tau (WT) and the three tau mutant proteins. All four tau proteins increased the frequency of projections at MT ends relative to controls lacking tau. Specifically, WT 4R tau induced projections at 39% of microtubule ends, compared with 7.4% in the no-tau control (Fig. 6*A*). The

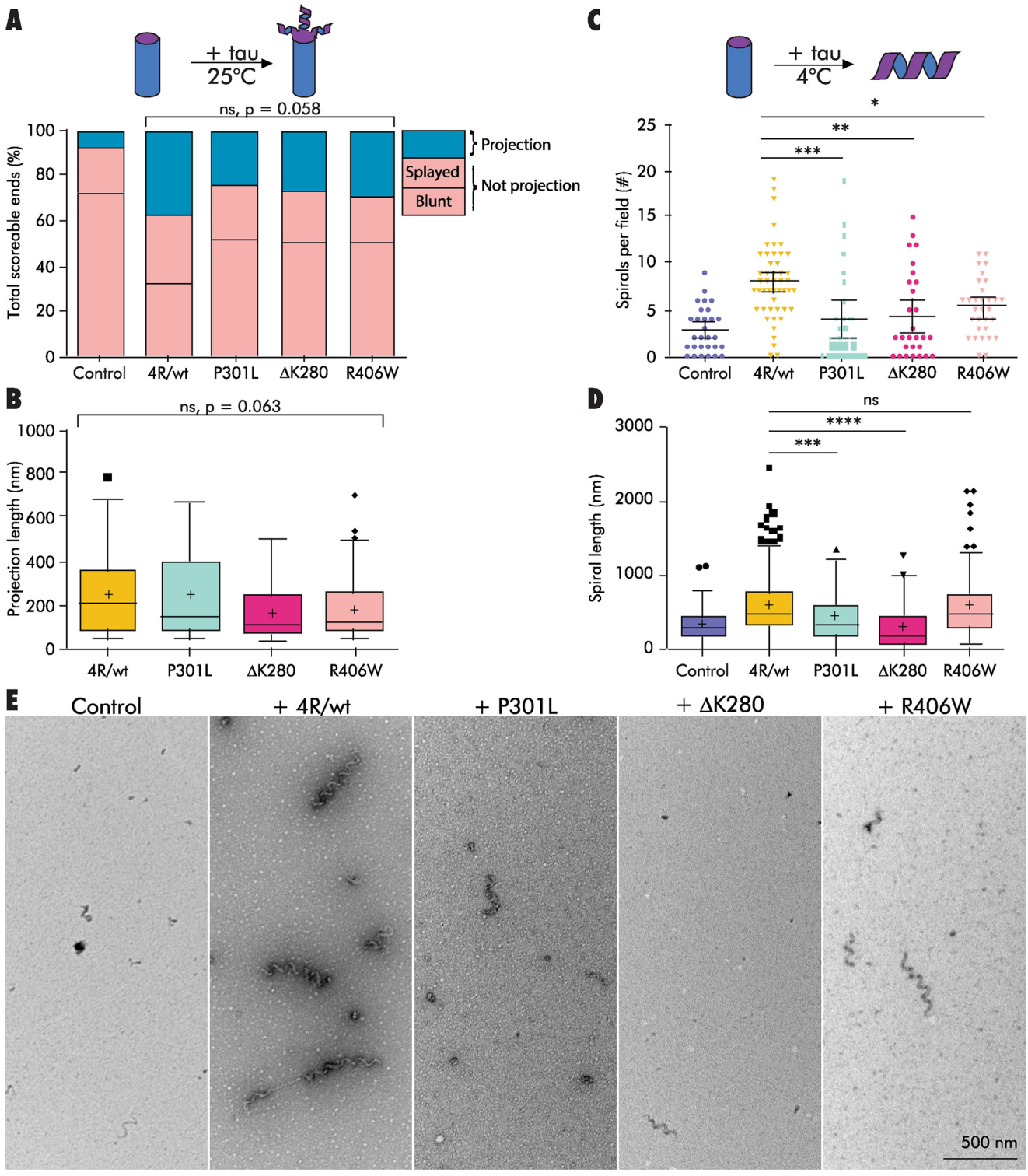


**Figure 6. FTDP-17 mutants show differential abilities to stabilize intermediate structures.** *A* and *B*, projection frequency (*A*) and length (*B*) after decoration of GMPCPP MTs (0.5 μM) with WT 4R tau (*4R/wt*; 10:1 tau/tubulin molar ratio) or tau with the FTDP-17–associated tau mutations P301L, ΔK280, or R406W. *C–E*, GMPCPP MTs (0.5 μM) disassembled in the presence of 4R/wt or FTDP-17 mutant tau (1:5 tau/tubulin molar ratio) differ in disassembly spiral abundance (*C*) and length (*D*). ****, $p < 0.0001$; ***, $p < 0.001$; **, $p < 0.01$; *, $p < 0.05$. *ns*, not significant, $p > 0.05$. See also Tables S6 and S7.

three mutants trended toward lower projection frequencies than WT (25, 26, and 29% of ends overall for P301L, ΔK280, and R406W, respectively; Fig. 6*A* and Table S6). These differences came close to but did not reach statistical significance (GLM $p = 0.058$). Projection length analysis showed that WT 4R tau stabilized projections with a mean length of 252 ± 24 nm (Fig. 6*B*). Although ΔK280 and R406W trended toward shorter mean projection lengths (171 ± 23 and 191 ± 21 nm, respectively), P301L projections (248 ± 38 nm) were similar to WT length, although there were no statistically significant differences between any mutant and WT (Welch's ANOVA $p = 0.06$).

Next, we asked whether the same tau mutants were able to stabilize disassembly spirals. GMPCPP MTs were diluted into cold buffer with or without each tau protein (final tubulin ~0.5 $\mu$M, 1:5 tau/tubulin molar ratio) and incubated at 4 °C for 10 min. WT 4R tau stabilized an average of 7.9 ± 0.6 spirals per field with a mean spiral length of 570 ± 18 nm, compared with 2.8 ± 0.5 spirals per field and a mean spiral length of 326 ± 30 nm in the no-tau controls (Fig. 6, *C–E*, and Table S7). All three tau mutants exhibited small but significant reductions in spirals per field relative to WT 4R tau (ANOVA $p = 0.0002$, Fig. 6, *C* and *E*). The ΔK280 and P301L mutants were more markedly compromised, with an average of 4.4 ± 0.9 spirals per field in ΔK280 and 3.9 ± 0.9 in P301L ($p = 0.0026$ and $p = 0.0007$ *versus* WT, respectively). Spiral lengths also differed among the tau mutants (Welch's ANOVA $p < 0.0001$). ΔK280 and P301L stabilized spirals with shorter mean lengths (297 ± 24 nm and 442 ± 27 nm, respectively) relative to WT 4R tau ($p < 0.0001$ and $p = 0.0004$). R406W, while still compromised compared with WT, appeared to be less affected than the other two mutants, stabilizing an average of 5.3 ± 0.5 spirals per field ($p = 0.027$ *versus* WT) that were no shorter than WT (579 ± 30 nm; Fig. 6*D* and Table S7). In summary, mutations ΔK280 and P301L negatively affect tau's ability to stabilize disassembly spirals in terms of both quantity and length, whereas the R406W mutation only negatively impacts spiral quantity.

## Discussion

The best understood role of tau in neuronal cell biology is to establish and maintain the proper regulation of MT dynamics, the growing and shortening events at MT ends. Proper regulation of these events is critical for many cellular functions, as evidenced by the deleterious effects of both MT-stabilizing and -destabilizing drugs (27). Indeed, one often suggested model for pathological tau action in Alzheimer's and related tauopathies is the destabilization of axonal MTs, leading to aberrant axonal transport and neuronal cell death (87, 88).

The simplest view of MT assembly involves the stepwise addition of individual tubulin dimer subunits onto the growing end of an MT (23). Indeed, measurements of incremental length increases on very-short time intervals (100 ms) during MT assembly using optical tweezers observed length increments of 8.1 nm (the length of a tubulin heterodimer) with only rare length increments greater than 16 nm (the length of two tubulin heterodimers) (23). Alternatively, other assembly data suggested that MT length fluctuates "on subsecond timescales, leading to apparent steps of 10–40 nm amplitude" (24), an observation that cannot be explained by the stochastic addition and subtraction of 8-nm dimers alone. Although the addition of tubulin oligomers rather than dimers at MT ends (89) has been proposed to explain this discrepancy, others favor a "dynamic GTP cap" model where rapid growth and shortening at the MT plus-end result in protofilaments containing unequal amounts of GTP-tubulin (25). This variation in cap size then adds to the overall variation in growth rate, as incoming dimers or oligomers, which have a greater surface area to interact with (*i.e.* more neighbors), will have a higher probability of forming productive lateral interactions, eventually resulting in straightening and incorporation into the growing MT lattice. By virtue of their curved morphology, GTP tubulin oligomers or protofilaments that have not yet been bound laterally on both sides may also provide a target for end-specific MAPs. Indeed, MAPs, including tau (47, 90), CLIP-170 (91), and EB1/3 (92), exhibit differential binding preferences based on the curvature of the tubulin.

We have used GMPCPP tubulin, which is widely used to mimic the pre-hydrolysis state of GTP tubulin, to explore effects of tau on MT assembly/disassembly structural intermediates that might otherwise be too transient to observe. We find that co-incubation of GMPCPP tubulin and tau resulted in the formation of tubulin spirals emanating (i) from the ends of pre-assembled MTs at 25 °C, (ii) from free tubulin heterodimers dimers at 4 °C, and (iii) from free tubulin heterodimers dimers at 34 °C. Spirals were also formed when MTs were disassembled by cold temperature in the presence of 4R tau. Importantly, all of these spiral structures were also observed, albeit at much lower frequencies, in the absence of tau and have also been observed in previous studies of both GTP and GMPCPP tubulin (62, 70, 82), consistent with the notion that that they are *bona fide* intermediates in the MT assembly/disassembly processes.

Furthermore, we find that 3R and 4R tau isoforms were similarly able to promote MT assembly intermediates but differ in their ability to stabilize disassembly intermediates, consistent with the well-established ability of 4R to suppress MT shortening events more effectively than does 3R tau (1, 13, 28, 35, 36, 81). Finally, we find that while three tau proteins harboring mutations that cause neurodegeneration and dementia were not compromised in their abilities to stabilize assembly intermediates (MT end projections), they were compromised in their abilities to stabilize disassembly intermediates (disassembly spirals). Collectively, our results indicate that stabilization of assembly/disassembly intermediates is a key feature of physiological tau action.

### *Intermediates in MT assembly, disassembly, and dynamics*

It has been proposed that the primary force at play within the MT lattice is outward longitudinal bending due to the intrinsic curvature of tubulin protofilaments. In general, MT lateral bonds are estimated to be ~5 times weaker in strength than longitudinal bonds (78, 93). As a result, the formation of these higher energy longitudinal bonds presents the larger barrier to MT nucleation, whereas the breakage of weaker lateral contacts between adjacent protofilaments at MT ends is believed to govern MT disassembly (78, 89, 93–95). Whereas a given region of tubulin heterodimers located within the main body of an MT is constrained in a straight conformation by lateral forces within the MT lattice on both sides, heterodimers/protofilaments near the MT end are less constrained structurally and may therefore realize some of their intrinsic curvature (96), resulting in the gently curving sheets observed at growing MT ends (68, 71, 76). Indeed, dynamic instability is thought to derive from the GTP hydrolysis event (and the resulting increased lattice strain) that occurs post-incorporation into the MT lattice. At a critical point following GTP hydrolysis, lateral bonds can break, and the liberated protofilament(s) can assume their intrinsic curvature and roll up, causing the straight and intact part of the tube to shorten. If the energy released by breaking lateral bonds at

MT ends is insufficient to propagate down the length of the tube, or the liberated protofilament(s) engages with some other stabilizing component (such as tau or other MAPs), the result will be a "meta-stable" intermediate state in which the MT end is energetically relaxed but not actively depolymerizing (96–100). This state defines a "rescue" event, when a depolymerizing MT switches to a paused or growth state. Thermal fluctuations may push MTs into or out of this meta-stable intermediate state, providing a possible explanation for the temperature dependence of rescue and catastrophe frequencies (96, 101). Janosi *et al.* (96) have proposed that a meta-stable intermediate is a potential point for regulation by MAPs through GTP–tubulin association and/or dissociation rate, intrinsic curvature, and/or cooperative binding.

The existence of intermediate states in MT assembly and disassembly was first described in early *in vitro* studies of MT nucleation and dynamics (61, 64, 70, 82, 102–104). Both rings and "twisted ribbon" (spiral) species form during MT nucleation in the presence of MAP-rich tubulin and GTP over the first ~4 min of assembly at 37 °C (64, 66, 82). These authors noted that the twisted ribbons/spirals would provide a more favorable intermediate state than rings, which would have to undergo opening into a single linear oligomer prior to incorporation at the growing MT end (40). Indeed, quantitative EM by Kirschner *et al.* (65) showed that ribbons were the predominant species in the first 30 s to 2 min after GTP addition, and their disappearance coincided with the appearance of increasing numbers of MTs.

Spirals have also been observed in the earliest phases (~30 s) (i) when free GMPCPP tubulin dimers are incubated at 4 °C in the presence of high concentrations of $Mg^{2+}$ (84), and (ii) when GMPCPP MTs are disassembled in the presence of high concentrations of $Ca^{2+}$ (70, 80). The Mg-induced spirals, which Wang *et al.* (84, 107) proposed are analogous to the outwardly-curved tubulin sheets observed at the ends of fast-growing GTP/GDP MTs *in vitro* using purified tubulin (68), in cell extracts (105), and in yeast (106), may constitute an intermediate structure during MT assembly. Different conditions, such as temperature, tubulin concentration, salt concentration, or the presence of MAPs, would be predicted to affect the equilibrium between sheet/MT elongation and sheet closure into MTs and could thereby affect global MT dynamics. For example, MAPs EB1 and EB3, which bind specifically to MT plus-ends and promote MT growth as well as both rescue and catastrophe, have been shown to increase tubulin sheet formation as well as to promote sheet closure into MTs (108, 109). Interestingly, EBs exhibit preferential binding for the post-hydrolysis but pre-phosphate release GDP-$P_i$ tubulin state (corresponding to the region immediately behind the GTP cap) but exhibit poor binding to GMPCPP MTs (110, 111).

Structural studies of the Mg-induced spirals described above revealed the existence of two types of lateral contacts, only one of which is present in the mature MT lattice (84, 107). It seems reasonable to suggest that tube closure requires the conversion of the non-MT mode of lateral contacts to the MT mode of contacts. We suspect that our tau-induced *de novo* spirals may possess similar types of lateral contacts as the Mg-induced spirals. The fact that our *de novo* spirals convert into intact MTs less effectively when warmed than do the Mg-induced spirals (84) suggests that tau may preferentially stabilize the non-MT lateral contacts. Wang *et al.* (84) note that the equilibrium between spiral and MT could be shifted based on the concentration of magnesium, with higher concentrations resulting in a longer time before conversion into MTs. In this regard, it is useful to recall that while Mg is normally necessary for MT assembly, it is not required for tau-mediated MT assembly (112). Additionally, it appears that the tau-mediated spirals are more stable than the Mg-induced spirals, because formation of the Mg-induced spirals requires higher GMPCPP tubulin concentrations (18–27 $\mu$M tubulin compared with 0.9 $\mu$M with tau) and higher magnesium concentrations than the corresponding tau-induced spirals (6–20 mM Mg *versus* 0.015–4.5 $\mu$M tau).

### *Implications for tau's mechanism of action*

The nature of the tau–MT interaction has been investigated for many years. Beginning with the acquisition of tau's amino acid sequence, Lee *et al.* (113) proposed that the "repeat region" of tau might serve as a microtubule-binding region, a hypothesis that was subsequently supported by direct experimental evidence (35, 114–116). Recent cryo-EM structural data (38), as well as several earlier studies, suggested that tau primarily stabilizes longitudinal tubulin–tubulin interactions (37, 41, 112). In contrast, several other studies have argued that tau primarily stabilizes lateral contacts between protofilaments (42, 90). Our biochemical data suggest that tau promotes both longitudinal and lateral interactions, as shown by longer spirals and projections (*i.e.* more longitudinal bonds), and more numerous spirals and projections (*i.e.* more protofilaments aligning together requires more lateral bonds) in tau-containing samples than in controls. Furthermore, as discussed above, our data suggest that tau may stabilize more than one type of lateral interaction.

How might these interactions mediate tau's effects on MT nucleation and the regulation of MT dynamics? Based on our observations and precedents in the literature, we suggest that tau promotes MT nucleation by first promoting the assembly and/or stabilization of longitudinal tubulin oligomers, which then associate laterally into small, slightly curved GTP–tubulin sheet- or spiral-like structures. It has been shown that tau can bind multiple tubulin dimers at once to form heterogeneous tau–tubulin "fuzzy" complexes that are positively correlated with the rate of MT assembly (57). These assembly intermediates might act as seeds and help to overcome the MT nucleation energy barrier. During MT growth, the sheet- or spiral-like structure may form on, or associate with, growing MT ends, forming new lateral interactions with other similar structures.

Our data suggest that promotion of tubulin sheet closure into an MT is not a tau-mediated event. The tau-stabilized spirals we observed, both at MT ends and free in solution, were inefficient at closing into MTs, especially under conditions promoting the formation of longer spirals (*e.g.* lower tau/tubulin molar ratios). Perhaps tubulin sheet closure is an intrinsic property of an MT end. In support of the latter perspective, control reactions containing only tubulin and no tau assemble efficiently into *bona fide* MTs. In contrast, the presence of tau in parallel reactions leads to abundant spirals and many fewer MTs. It is notable that at low concentrations, 4R tau exhibits a much

stronger effect on the suppression of MT catastrophe (~30-fold) than it does on the promotion of MT growth (~1.5-fold). Perhaps tau primarily serves to promote assembly and/or stabilization of spirals, an otherwise unstable intermediate that could either move toward tube closure by an intrinsic mechanism or rapid disassembly. This would also be consistent with the observations that addition of tau to MTs at steady state leads to a marked increase in the percentage of MTs that are neither growing nor shortening (29).

Finally, our disassembly experiments indicate that 4R tau more effectively stabilizes intermediates generated during MT disassembly than does 3R tau. The mechanisms underlying these differential activities remain unclear. We speculate that the differences may arise from the differential importance of lateral and/or longitudinal bonds in MT assembly and disassembly contexts. For example, 3R tau may be less efficient than 4R tau at stabilizing MT-specific lateral contacts, which would be predicted to primarily affect MT disassembly. Alternatively, the relatively equal abilities of both 3R and 4R tau to promote MT nucleation and assembly may derive from the promotion of longitudinal bonds and possibly also the non-MT type of lateral contacts.

The fact that the ability to stabilize disassembly intermediates appears to be compromised in three well-characterized mutant tau variants suggests that the loss of this ability may contribute to pathological tau action.

## Experimental procedures

### *Purification of tau and tubulin*

cDNA expression vectors (pRK) encoding human tau isoforms (2N3R, 0N4R, and 2N4R) were kind gifts from Dr. Kenneth Kosik (University of California Santa Barbara) and Dr. Gloria Lee (Iowa State University). All tau constructs possessed both alternatively spliced, amino end exons ("2N") except for the pathological tau mutants, which possessed none of the amino end inserts ("0N"). For experiments involving use of FTDP-17 mutants, 0N4R tau was used as the WT control because the mutations were in 0N4R background. Prior to experiments with mutants, experiments were performed to verify that 0N4R produced end projections and stabilized disassembly spirals to the same extent as 2N4R tau (data not shown). FTDP-17 tau mutation constructs (ΔK280, P301L, and R406W) were generated as described in Ref. 18 from the 0N4R WT construct by QuikChange site-directed mutagenesis (Stratagene). All mutations were verified by DNA sequence analysis.

Tau was expressed and purified according to standard procedures described in Ref. 117. Briefly, tau was expressed in BL21(DE3) pLacI cells (Invitrogen). Bacteria were lysed by a French press, boiled for 10 min, and then passed over a phosphocellulose column. Tau-containing fractions were subsequently pooled and then further purified using hydrophobic interaction column chromatography (HisTrap Phenyl HP, GE Healthcare). Fractions containing pure tau were then pooled, concentrated, and buffer-exchanged into Na-BRB80 buffer (80 mM PIPES, 1 mM EGTA, 1 mM $MgSO_4$, pH 6.8, with NaOH) and stored at −80 °C. Concentration was determined by SDS-PAGE comparison with a tau mass standard, the concentration of which had been established by MS amino acid analysis (13).

Tubulin was purified as described in Ref. 118 from bovine brain by three cycles of assembly and disassembly. Further separation of tubulin from microtubule-associated proteins was achieved by elution through a phosphocellulose column equilibrated with 50 mM PIPES, 1 mM $MgSO_4$, 1 mM EGTA, 0.1 mM GTP, pH 6.8. Purified tubulin (>99% pure) was drop-frozen in liquid nitrogen and stored at −80 °C. All tubulin concentrations in this paper refer to the heterodimer (mass = 110,000 Da).

### *Preparation of GMPCPP microtubules*

GMPCPP microtubules were made as described in Ref. 33. Briefly, purified tubulin (20 μM) was assembled in the presence of 1 mM GMPCPP (GpCpp; Jena Bioscience) for 30 min at 34 °C. The resulting microtubules were collected by centrifugation (52,000 × *g*, 25 °C, 12 min). To remove any residual GTP remaining in the microtubule lattice, microtubules were then depolymerized on ice, followed by a second warm assembly in buffer containing GMPCPP (0.5 mM). These GMPCPP microtubules were collected by centrifugation (12 min, 52,000 × *g*, 4 °C), gently resuspended in warm K-BRB80 buffer (80 mM PIPES, 1 mM EGTA, 1 mM $MgSO_4$, pH 6.8, with KOH), and then flash-frozen in liquid nitrogen and stored at −80 °C in single-use aliquots.

### *GMPCPP microtubule decoration with tau*

Just prior to each experiment, a fresh tube of the GMPCPP microtubule stock was immediately transferred to a 34 °C water bath for 10 min in order to recover from the frozen state. Microtubules were then diluted into warm assay buffer (80 mM PIPES, 1 mM EGTA, 1 mM $MgSO_4$, pH 6.8, with KOH) supplemented with 1 mM DTT. Tau was thawed on ice and then warmed to 25 °C immediately prior to the experiment. Diluted microtubules were added to samples containing tau or buffer and incubated for 10 min at 25 °C.

### *Formation of GMPCPP tubulin de novo spirals*

GMPCPP microtubule stocks were removed from storage at −80 °C and immediately placed on ice for 30 min to depolymerize. This depolymerized tubulin was then diluted to an appropriate working concentration (~0.9 μM) with cold K-BRB80 supplemented with 1 mM DTT. This working dilution was then added to cold solutions of tau or tau buffer, mixed gently, and co-incubated on ice for an additional 30 min. For experiments using higher tubulin concentrations, MTs were prepared fresh, as indicated above, immediately prior to the experiment and then were diluted to the appropriate concentration as needed.

### *Formation of GMPCPP tubulin disassembly spirals*

GMPCPP microtubules were removed from the freezer, incubated for 10 min at 34 °C, and then diluted into warm assay buffer as above. Microtubules were then added to cold tau or buffer and incubated at 4 °C for 10 min. For experiments at higher tubulin concentrations, GMPCPP microtubules were prepared fresh as above, added to 25 °C tau or buffer, and then chilled to 4 °C for 60 min.

### TEM

Samples were fixed with glutaraldehyde (0.2% final), applied to grids (200 mesh Formvar/carbon/copper, Electron Microscopy Sciences), coated with cytochrome *c*, and then stained with uranyl acetate (1% final). Grids were randomly imaged at ×2500 (for microtubule length measurements) and ×30,000 (for end scoring, projection, and spiral measurements) magnifications using a JEOL 1230 transmission electron microscope (80 kV) and AMT image capture software. Images were then coded and analyzed blind to prevent investigator bias. At least 50 microtubule ends per sample were scored for all decoration experiments.

### Statistical analysis

Statistics were performed using RStudio (version 1.1.423 (RCore Team, 2018; RStudio Team, 2018)), JMP (JMP Pro 14), and Statistics101 (version 4.7). Note that exact $p$ values are only reported for $p \geq 0.0001$.

*Author contributions*—R. L. B., N. E. L., L. W., and S. C. F. conceptualization; R. L. B., N. E. L., J. L., K. R., M. F. S., L. W., and S. C. F. data curation; R. L. B., N. E. L., J. L., M. F. S., and S. C. F. formal analysis; R. L. B., N. E. L., J. L., K. R., M. F. S., L. W., and S. C. F. investigation; R. L. B. visualization; R. L. B., N. E. L., K. R., M. F. S., L. W., and S. C. F. methodology; R. L. B., N. E. L., L. W., and S. C. F. writing-original draft; R. L. B., N. E. L., L. W., and S. C. F. writing-review and editing; L. W. and S. C. F. project administration; S. C. F. supervision; S. C. F. funding acquisition.

*Acknowledgments—We thank Herb Miller for generously providing purified bovine tubulin, Colleen Sweeney for help with data analysis, Geoff Lewis for TEM assistance, MaryAnn Jordan for valuable discussion, and William Rice for advice on statistical approaches and for custom JMP analysis programs. We acknowledge the use of the NRI-MCDB Microscopy Facility.*

## References


1. Bunker, J. M., Wilson, L., Jordan, M. A., and Feinstein, S. C. (2004) Modulation of microtubule dynamics by tau in living cells: implications for development and neurodegeneration. *Mol. Biol. Cell* **15,** 2720–2728
2. Drubin, D. G., and Kirschner, M. W. (1986) Tau protein function in living cells. *J. Cell Biol.* **103,** 2739–2746 CrossRef Medline
3. Drubin, D. G., Feinstein, S. C., Shooter, E. M., and Kirschner, M. W. (1985) Nerve growth factor-induced neurite outgrowth in PC12 cells involves the coordinate induction of microtubule assembly and assembly-promoting factors. *J. Cell Biol.* **101,** 1799–1807 CrossRef Medline
4. Caceres, A., and Kosik, K. S. (1990) Inhibition of neurite polarity by tau antisense oligonucleotides in primary cerebellar neurons. *Nature* **343,** 461–463 CrossRef Medline
5. Esmaeli-Azad, B., McCarty, J. H., and Feinstein, S. C. (1994) Sense and antisense transfection analysis of tau function: tau influences net microtubule assembly, neurite outgrowth and neuritic stability. *J. Cell Sci.* **107,** 869–879 Medline
6. Liu, C. W., Lee, G., and Jay, D. G. (1999) Tau is required for neurite outgrowth and growth cone motility of chick sensory neurons. *Cell Motil. Cytoskeleton* **43,** 232–242 CrossRef Medline
7. Stamer, K., Vogel, R., Thies, E., Mandelkow, E., and Mandelkow, E. M. (2002) Tau blocks traffic of organelles, neurofilaments, and APP vesicles in neurons and enhances oxidative stress. *J. Cell Biol.* **156,** 1051–1063 CrossRef Medline
8. Harada, A., Oguchi, K., Okabe, S., Kuno, J., Terada, S., Ohshima, T., Sato-Yoshitake, R., Takei, Y., Noda, T., and Hirokawa, N. (1994) Altered microtubule organization in small-calibre axons of mice lacking tau protein. *Nature* **369,** 488–491 CrossRef Medline
9. Takei, Y., Teng, J., Harada, A., and Hirokawa, N. (2000) Defects in axonal elongation and neuronal migration in mice with disrupted tau and map1b genes. *J. Cell Biol.* **150,** 989–1000 CrossRef Medline
10. Garcia, M. L., and Cleveland, D. W. (2001) Going new places using an old MAP: tau, microtubules and human neurodegenerative disease. *Curr. Opin. Cell Biol.* **13,** 41–48 CrossRef Medline
11. Wolfe, M. S. (2009) Tau mutations in neurodegenerative diseases. *J. Biol. Chem.* **284,** 6021–6025 CrossRef Medline
12. Wang, Y., and Mandelkow, E. (2016) Tau in physiology and pathology. *Nat. Rev. Neurosci.* **17,** 5–21 CrossRef Medline
13. Panda, D., Samuel, J. C., Massie, M., Feinstein, S. C., and Wilson, L. (2003) Differential regulation of microtubule dynamics by three- and four-repeat tau: implications for the onset of neurodegenerative disease. *Proc. Natl. Acad. Sci. U.S.A.* **100,** 9548–9553 CrossRef Medline
14. Feinstein, S. C., and Wilson, L. (2005) Inability of tau to properly regulate neuronal microtubule dynamics: a loss–of–function mechanism by which tau might mediate neuronal cell death. *Biochim. Biophys. Acta* **1739,** 268–279 CrossRef Medline
15. Goedert, M., and Spillantini, M. G. (2000) Tau mutations in frontotemporal dementia FTDP-17 and their relevance for Alzheimer's disease. *Biochim. Biophys. Acta* **1502,** 110–121 CrossRef Medline
16. DeTure, M., Ko, L. W., Yen, S., Nacharaju, P., Easson, C., Lewis, J., van Slegtenhorst, M., Hutton, M., and Yen, S. H. (2000) Missense tau mutations identified in FTDP-17 have a small effect on tau–microtubule interactions. *Brain Res.* **853,** 5–14 CrossRef Medline
17. Bunker, J. M., Kamath, K., Wilson, L., Jordan, M. A., and Feinstein, S. C. (2006) FTDP-17 mutations compromise the ability of tau to regulate microtubule dynamics in cells. *J. Biol. Chem.* **281,** 11856–11863 CrossRef Medline
18. LeBoeuf, A. C., Levy, S. F., Gaylord, M., Bhattacharya, A., Singh, A. K., Jordan, M. A., Wilson, L., and Feinstein, S. C. (2008) FTDP-17 mutations in Tau alter the regulation of microtubule dynamics: an "alternative core" model for normal and pathological Tau action. *J. Biol. Chem.* **283,** 36406–36415 CrossRef Medline
19. Nagiec, E. W., Sampson, K. E., and Abraham, I. (2001) Mutated tau binds less avidly to microtubules than wildtype tau in living cells. *J. Neurosci. Res.* **63,** 268–275 CrossRef Medline
20. Hong, M., Zhukareva, V., Vogelsberg-Ragaglia, V., Wszolek, Z., Reed, L., Miller, B. I., Geschwind, D. H., Bird, T. D., McKeel, D., Goate, A., Morris, J. C., Wilhelmsen, K. C., Schellenberg, G. D., Trojanowski, J. Q., and Lee, V. M. (1998) Mutation-specific functional impairments in distinct tau isoforms of hereditary FTDP-17. *Science* **282,** 1914–1917 CrossRef Medline
21. Lewis, J., McGowan, E., Rockwood, J., Melrose, H., Nacharaju, P., Van Slegtenhorst, M., Gwinn-Hardy, K., Paul Murphy, M., Baker, M., Yu, X., Duff, K., Hardy, J., Corral, A., Lin, W. L., Yen, S. H., *et al.* (2000) Neurofibrillary tangles, amyotrophy and progressive motor disturbance in mice expressing mutant (P301L) tau protein. *Nat. Genet.* **25,** 402–405 CrossRef Medline
22. Combs, B., and Gamblin, T. C. (2012) FTDP-17 Tau mutations induce distinct effects on aggregation and microtubule interactions. *Biochemistry* **51,** 8597–8607 CrossRef Medline
23. Schek, H. T., 3rd., Gardner, M. K., Cheng, J., Odde, D. J., and Hunt, A. J. (2007) Microtubule assembly dynamics at the nanoscale. *Curr. Biol.* **17,** 1445–1455 CrossRef Medline
24. Kerssemakers, J. W., Munteanu, E. L., Laan, L., Noetzel, T. L., Janson, M. E., and Dogterom, M. (2006) Assembly dynamics of microtubules at molecular resolution. *Nature* **442,** 709–712 CrossRef Medline
25. Howard, J., and Hyman, A. A. (2009) Growth, fluctuation and switching at microtubule plus-ends. *Nat. Rev. Mol. Cell Biol.* **10,** 569–574 CrossRef Medline
26. Drechsel, D. N., Hyman, A. A., Cobb, M. H., and Kirschner, M. W. (1992) Modulation of the dynamic instability of tubulin assembly by the microtubule-associated protein tau. *Mol. Biol. Cell* **3,** 1141–1154 CrossRef Medline
27. Jordan, M. A., and Wilson, L. (2004) Microtubules as a target for anticancer drugs. *Nat. Rev. Cancer* **4,** 253–265 CrossRef Medline

28. Gustke, N., Trinczek, B., Biernat, J., Mandelkow, E. M., and Mandelkow, E. (1994) Domains of Tau-protein and interactions with microtubules. *Biochemistry* **33,** 9511–9522 CrossRef Medline
29. Panda, D., Goode, B. L., Feinstein, S. C., and Wilson, L. (1995) Kinetic stabilization of microtubule dynamics at steady state by tau and microtubule-binding domains of tau. *Biochemistry* **34,** 11117–11127 CrossRef Medline
30. Goedert, M., Spillantini, M. G., Jakes, R., Rutherford, D., and Crowther, R. A. (1989) Multiple isoforms of human microtubule-associated protein tau: sequences and localization in neurofibrillary tangles of Alzheimer's disease. *Neuron* **3,** 519–526 CrossRef Medline
31. Spillantini, M. G., Van Swieten, J. C., and Goedert, M. (2000) Tau gene mutations in frontotemporal dementia and parkinsonism linked to chromosome 17 (FTDP-17). *Neurogenetics* **2,** 193–205 CrossRef Medline
32. Spillantini, M. G., Murrell, J. R., Goedert, M., Farlow, M. R., Klug, A., and Ghetti, B. (1998) Mutation in the tau gene in familial multiple system tauopathy with presenile dementia. *Proc. Natl. Acad. Sci. U.S.A.* **95,** 7737–7741 CrossRef Medline
33. Stumpff, J., Cooper, J., Domnitz, S., Moore, A. T., Rankin, K. E., Wagenbach, M., and Wordeman, L. (2007) *In vitro* and *in vivo* analysis of microtubule-destabilizing kinesins. *Methods Mol. Biol.* **392,** 37–49 CrossRef Medline
34. Cleveland, D. W., Hwo, S. Y., and Kirschner, M. W. (1977) Purification of tau, a microtubule-associated protein that induces assembly of microtubules from purified tubulin. *J. Mol. Biol.* **116,** 207–225 CrossRef Medline
35. Trinczek, B., Biernat, J., Baumann, K., Mandelkow, E. M., and Mandelkow, E. (1995) Domains of tau protein, differential phosphorylation, and dynamic instability of microtubules. *Mol. Biol. Cell* **6,** 1887–1902 CrossRef Medline
36. Levy, S. F., Leboeuf, A. C., Massie, M. R., Jordan, M. A., Wilson, L., and Feinstein, S. C. (2005) Three- and four-repeat tau regulate the dynamic instability of two distinct microtubule subpopulations in qualitatively different manners. Implications for neurodegeneration. *J. Biol. Chem.* **280,** 13520–13528 CrossRef Medline
37. Al-Bassam, J., Ozer, R. S., Safer, D., Halpain, S., and Milligan, R. A. (2002) MAP2 and tau bind longitudinally along the outer ridges of microtubule protofilaments. *J. Cell Biol.* **157,** 1187–1196 CrossRef Medline
38. Kellogg, E. H., Hejab, N. M. A., Poepsel, S., Downing, K. H., DiMaio, F., and Nogales, E. (2018) Near-atomic model of microtubule–tau interactions. *Science* **360,** 1242–1246 CrossRef Medline
39. Santarella, R. A., Skiniotis, G., Goldie, K. N., Tittmann, P., Gross, H., Mandelkow, E. M., Mandelkow, E., and Hoenger, A. (2004) Surface-decoration of microtubules by human tau. *J. Mol. Biol.* **339,** 539–553 CrossRef Medline
40. Kutter, S., Eichner, T., Deaconescu, A. M., and Kern, D. (2016) Regulation of microtubule assembly by tau and not by Pin1. *J. Mol. Biol.* **428,** 1742–1759 CrossRef Medline
41. Kadavath, H., Hofele, R. V., Biernat, J., Kumar, S., Tepper, K., Urlaub, H., Mandelkow, E., and Zweckstetter, M. (2015) Tau stabilizes microtubules by binding at the interface between tubulin heterodimers. *Proc. Natl. Acad. Sci. U.S.A.* **112,** 7501–7506 CrossRef Medline
42. Kar, S., Fan, J., Smith, M. J., Goedert, M., and Amos, L. A. (2003) Repeat motifs of tau bind to the insides of microtubules in the absence of taxol. *EMBO J.* **22,** 70–77 CrossRef Medline
43. Martinho, M., Allegro, D., Huvent, I., Chabaud, C., Etienne, E., Kovacic, H., Guigliarelli, B., Peyrot, V., Landrieu, I., Belle, V., and Barbier, P. (2018) Two Tau-binding sites on tubulin revealed by thiol-disulfide exchanges. *Sci. Rep.* **8,** 13846 CrossRef Medline
44. Makrides, V., Massie, M. R., Feinstein, S. C., and Lew, J. (2004) Evidence for two distinct binding sites for tau on microtubules. *Proc. Natl. Acad. Sci. U.S.A.* **101,** 6746–6751 CrossRef Medline
45. Breuzard, G., Hubert, P., Nouar, R., De Bessa, T., Devred, F., Barbier, P., Sturgis, J. N., and Peyrot, V. (2013) Molecular mechanisms of Tau binding to microtubules and its role in microtubule dynamics in live cells. *J. Cell Sci.* **126,** 2810–2819 CrossRef Medline
46. Konzack, S., Thies, E., Marx, A., Mandelkow, E. M., and Mandelkow, E. (2007) Swimming against the tide: mobility of the microtubule-associated protein tau in neurons. *J. Neurosci.* **27,** 9916–9927 CrossRef Medline
47. Samsonov, A., Yu, J. Z., Rasenick, M., and Popov, S. V. (2004) Tau interaction with microtubules *in vivo*. *J. Cell Sci.* **117,** 6129–6141 CrossRef Medline
48. Janning, D., Igaev, M., Sündermann, F., Brühmann, J., Beutel, O., Heinisch, J. J., Bakota, L., Piehler, J., Junge, W., and Brandt, R. (2014) Single-molecule tracking of tau reveals fast kiss-and-hop interaction with microtubules in living neurons. *Mol. Biol. Cell* **25,** 3541–3551 CrossRef Medline
49. Hinrichs, M. H., Jalal, A., Brenner, B., Mandelkow, E., Kumar, S., and Scholz, T. (2012) Tau protein diffuses along the microtubule lattice. *J. Biol. Chem.* **287,** 38559–38568 CrossRef Medline
50. Hirokawa, N., Shiomura, Y., and Okabe, S. (1988) Tau proteins: the molecular structure and mode of binding on microtubules. *J. Cell Biol.* **107,** 1449–1459 CrossRef Medline
51. Kim, H., Jensen, C. G., and Rebhun, L. I. (1986) The binding of MAP-2 and tau on brain microtubules *in vitro*: implications for microtubule structure. *Ann. N.Y. Acad. Sci.* **466,** 218–239 CrossRef Medline
52. Wilson, L., Jordan, M. A., Morse, A., and Margolis, R. L. (1982) Interaction of vinblastine with steady-state microtubules *in vitro*. *J. Mol. Biol.* **159,** 125–149 CrossRef Medline
53. Singer, W. D., Jordan, M. A., Wilson, L., and Himes, R. H. (1989) Binding of vinblastine to stabilized microtubules. *Mol. Pharmacol.* **36,** 366–370 Medline
54. Gigant, B., Wang, C., Ravelli, R. B., Roussi, F., Steinmetz, M. O., Curmi, P. A., Sobel, A., and Knossow, M. (2005) Structural basis for the regulation of tubulin by vinblastine. *Nature* **435,** 519–522 CrossRef Medline
55. Jordan, M. A., Margolis, R. L., Himes, R. H., and Wilson, L. (1986) Identification of a distinct class of vinblastine-binding sites on microtubules. *J. Mol. Biol.* **187,** 61–73 CrossRef Medline
56. Li, X. H., Culver, J. A., and Rhoades, E. (2015) Tau binds to multiple tubulin dimers with helical structure. *J. Am. Chem. Soc.* **137,** 9218–9221 CrossRef Medline
57. Li, X. H., and Rhoades, E. (2017) Heterogeneous Tau–tubulin complexes accelerate microtubule polymerization. *Biophys. J.* **112,** 2567–2574 CrossRef Medline
58. Sontag, E., Nunbhakdi-Craig, V., Lee, G., Brandt, R., Kamibayashi, C., Kuret, J., White C. L., 3rd, Mumby, M. C., and Bloom, G. S. (1999) Molecular interactions among protein phosphatase 2A, tau, and microtubules. Implications for the regulation of tau phosphorylation and the development of tauopathies. *J. Biol. Chem.* **274,** 25490–25498 CrossRef Medline
59. Roostalu, J., and Surrey, T. (2017) Microtubule nucleation: beyond the template. *Nat. Rev. Mol. Cell Biol.* **18,** 702–710 CrossRef Medline
60. Erickson, H. P., and Voter, W. A. (1986) Nucleation of microtubule assembly. Experimental kinetics, computer fitting of models, and observations on tubulin rings. *Ann. N.Y. Acad. Sci.* **466,** 552–565 CrossRef Medline
61. Sandoval, I. V., and Weber, K. (1980) Different tubulin polymers are produced by microtubule-associated proteins MAP2 and tau in the presence of guanosine 5′-(α,β-methylene)triphosphate. *J. Biol. Chem.* **255,** 8952–8954 Medline
62. Sandoval, I. V., and Weber, K. (1980) Guanosine 5′-(α,β-methylene)-triphosphate enhances specifically microtubule nucleation and stops the treadmill of tubulin protomers. *J. Biol. Chem.* **255,** 6966–6974 Medline
63. Frigon, R. P., and Timasheff, S. N. (1975) Magnesium-induced self-association of calf brain tubulin. Stoichiometry. *Biochemistry* **14,** 4559–4566 CrossRef Medline
64. Erickson, H. P. (1974) Assembly of microtubules from preformed, ring-shaped protofilaments and 6-S tubulin. *J. Supramol. Struct.* **2,** 393–411 CrossRef Medline
65. Kirschner, M. W., Suter, M., Weingarten, M., and Littman, D. (1975) The role of rings in the assembly of microtubules *in vitro*. *Ann. N.Y. Acad. Sci.* **253,** 90–106 CrossRef Medline
66. Voter, W. A., and Erickson, H. P. (1984) The kinetics of microtubule assembly. Evidence for a two-stage nucleation mechanism. *J. Biol. Chem.* **259,** 10430–10438 Medline
67. Caudron, N., Arnal, I., Buhler, E., Job, D., and Valiron, O. (2002) Microtubule nucleation from stable tubulin oligomers. *J. Biol. Chem.* **277,** 50973–50979 CrossRef Medline

68. Chrétien, D., Fuller, S. D., and Karsenti, E. (1995) Structure of growing microtubule ends: two-dimensional sheets close into tubes at variable rates. *J. Cell Biol.* **129,** 1311–1328 CrossRef Medline
69. Kirschner, M. W., and Mitchison, T. (1986) Microtubule dynamics. *Nature* **324,** 621 CrossRef Medline
70. Müller-Reichert, T., Chrétien, D., Severin, F., and Hyman, A. A. (1998) Structural changes at microtubule ends accompanying GTP hydrolysis: information from a slowly hydrolyzable analogue of GTP, guanylyl ($\alpha,\beta$)methylenediphosphonate. *Proc. Natl. Acad. Sci. U.S.A.* **95,** 3661–3666 CrossRef Medline
71. Hyman, A. A., Chrétien, D., Arnal, I., and Wade, R. H. (1995) Structural changes accompanying GTP hydrolysis in microtubules: information from a slowly hydrolyzable analogue guanylyl ($\alpha,\beta$)-methylenediphosphonate. *J. Cell Biol.* **128,** 117–125 CrossRef Medline
72. Brouhard, G. J., and Rice, L. M. (2014) The contribution of $\alpha\beta$-tubulin curvature to microtubule dynamics. *J. Cell Biol.* **207,** 323–334 CrossRef Medline
73. Alushin, G. M., Lander, G. C., Kellogg, E. H., Zhang, R., Baker, D., and Nogales, E. (2014) High-resolution microtubule structures reveal the structural transitions in $\alpha\beta$-tubulin upon GTP hydrolysis. *Cell* **157,** 1117–1129 CrossRef Medline
74. Rice, L. M., Montabana, E. A., and Agard, D. A. (2008) The lattice as allosteric effector: structural studies of $\alpha\beta$- and $\gamma$-tubulin clarify the role of GTP in microtubule assembly. *Proc. Natl. Acad. Sci. U.S.A.* **105,** 5378–5383 CrossRef Medline
75. Zhang, R., Alushin, G. M., Brown, A., and Nogales, E. (2015) Mechanistic origin of microtubule dynamic instability and its modulation by EB proteins. *Cell* **162,** 849–859 CrossRef Medline
76. Hyman, A. A., Salser, S., Drechsel, D. N., Unwin, N., and Mitchison, T. J. (1992) Role of GTP hydrolysis in microtubule dynamics: information from a slowly hydrolyzable analogue, GMPCPP. *Mol. Biol. Cell* **3,** 1155–1167 CrossRef Medline
77. Elie-Caille, C., Severin, F., Helenius, J., Howard, J., Muller, D. J., and Hyman, A. A. (2007) Straight GDP-tubulin protofilaments form in the presence of taxol. *Curr. Biol.* **17,** 1765–1770 CrossRef Medline
78. Mandelkow, E. M., Mandelkow, E., and Milligan, R. A. (1991) Microtubule dynamics and microtubule caps: a time-resolved cryo-electron microscopy study. *J. Cell Biol.* **114,** 977–991 CrossRef Medline
79. Sandoval, I. V., MacDonald, E., Jameson, J. L., and Cuatrecasas, P. (1977) Role of nucleotides in tubulin polymerization: effect of guanylyl 5′-methylenediphosphonate. *Proc. Natl. Acad. Sci. U.S.A.* **74,** 4881–4885 CrossRef Medline
80. Sandoval, I. V., Jameson, J. L., Niedel, J., MacDonald, E., and Cuatrecasas, P. (1978) Role of nucleotides in tubulin polymerization: effect of guanosine 5′-methylene diphosphonate. *Proc. Natl. Acad. Sci. U.S.A.* **75,** 3178–3182 CrossRef Medline
81. Goode, B. L., Chau, M., Denis, P. E., and Feinstein, S. C. (2000) Structural and functional differences between 3-repeat and 4-repeat tau isoforms. Implications for normal tau function and the onset of neurodegenerative disease. *J. Biol. Chem.* **275,** 38182–38189 CrossRef Medline
82. Kirschner, M. W., Honig, L. S., and Williams, R. C. (1975) Quantitative electron microscopy of microtubule assembly *in vitro*. *J. Mol. Biol.* **99,** 263–276 CrossRef Medline
83. Kirschner, M. W., and Williams, R. C. (1974) The mechanism of microtubule assembly *in vitro*. *J. Supramol. Struct.* **2,** 412–428 CrossRef Medline
84. Wang, H. W., Long, S., Finley, K. R., and Nogales, E. (2005) Assembly of GMPCPP-bound tubulin into helical ribbons and tubes and effect of colchicine. *Cell Cycle* **4,** 1157–1160 CrossRef Medline
85. Karr, T. L., Kristofferson, D., and Purich, D. L. (1980) Mechanism of microtubule depolymerization. Correlation of rapid induced disassembly experiments with a kinetic model for endwise depolymerization. *J. Biol. Chem.* **255,** 8560–8566 Medline
86. Barghorn, S., Zheng-Fischhöfer, Q., Ackmann, M., Biernat, J., von Bergen, M., Mandelkow, E. M., and Mandelkow, E. (2000) Structure, microtubule interactions, and paired helical filament aggregation by tau mutants of frontotemporal dementias. *Biochemistry* **39,** 11714–11721 CrossRef Medline
87. Stokin, G. B., and Goldstein, L. S. (2006) Axonal transport and Alzheimer's disease. *Annu. Rev. Biochem.* **75,** 607–627 CrossRef Medline
88. Brunden, K. R., Lee, V. M., Smith, A. B., 3rd, Trojanowski, J. Q., and Ballatore, C. (2017) Altered microtubule dynamics in neurodegenerative disease: therapeutic potential of microtubule-stabilizing drugs. *Neurobiol. Dis.* **105,** 328–335 CrossRef Medline
89. Mozziconacci, J., Sandblad, L., Wachsmuth, M., Brunner, D., and Karsenti, E. (2008) Tubulin dimers oligomerize before their incorporation into microtubules. *PLoS ONE* **3,** e3821 CrossRef Medline
90. Duan, A. R., Jonasson, E. M., Alberico, E. O., Li, C., Scripture, J. P., Miller, R. A., Alber, M. S., and Goodson, H. V. (2017) Interactions between Tau and different conformations of tubulin: implications for tau function and mechanism. *J. Mol. Biol.* **429,** 1424–1438 CrossRef Medline
91. Arnal, I., Heichette, C., Diamantopoulos, G. S., and Chrétien, D. (2004) CLIP-170/tubulin-curved oligomers coassemble at microtubule ends and promote rescues. *Curr. Biol.* **14,** 2086–2095 CrossRef Medline
92. Guesdon, A., Bazile, F., Buey, R. M., Mohan, R., Monier, S., García, R. R., Angevin, M., Heichette, C., Wieneke, R., Tampé, R., Duchesne, L., Akhmanova, A., Steinmetz, M. O., and Chrétien, D. (2016) EB1 interacts with outwardly curved and straight regions of the microtubule lattice. *Nat. Cell Biol.* **18,** 1102–1108 CrossRef Medline
93. VanBuren, V., Odde, D. J., and Cassimeris, L. (2002) Estimates of lateral and longitudinal bond energies within the microtubule lattice. *Proc. Natl. Acad. Sci. U.S.A.* **99,** 6035–6040 CrossRef Medline
94. Sept, D., Baker, N. A., and McCammon, J. A. (2003) The physical basis of microtubule structure and stability. *Protein Sci.* **12,** 2257–2261 CrossRef Medline
95. Margolin, G., Gregoretti, I. V., Cickovski, T. M., Li, C., Shi, W., Alber, M. S., and Goodson, H. V. (2012) The mechanisms of microtubule catastrophe and rescue: implications from analysis of a dimer-scale computational model. *Mol. Biol. Cell* **23,** 642–656 CrossRef Medline
96. Jánosi, I. M., Chrétien, D., and Flyvbjerg, H. (2002) Structural microtubule cap: stability, catastrophe, rescue, and third state. *Biophys. J.* **83,** 1317–1330 CrossRef Medline
97. Tran, P. T., Walker, R. A., and Salmon, E. D. (1997) A metastable intermediate state of microtubule dynamic instability that differs significantly between plus and minus-ends. *J. Cell Biol.* **138,** 105–117 CrossRef Medline
98. Waterman-Storer, C. M., and Salmon, E. D. (1997) Microtubule dynamics: treadmilling comes around again. *Curr. Biol.* **7,** R369–372 CrossRef Medline
99. Odde, D. J., Ma, L., Briggs, A. H., DeMarco, A., and Kirschner, M. W. (1999) Microtubule bending and breaking in living fibroblast cells. *J. Cell Sci.* **112,** 3283–3288 Medline
100. Vorobjev, I. A., Svitkina, T. M., and Borisy, G. G. (1997) Cytoplasmic assembly of microtubules in cultured cells. *J. Cell Sci.* **110,** 2635–2645 Medline
101. Fygenson, D. K., Braun, E., and Libchaber, A. (1994) Phase diagram of microtubules. *Phys. Rev. E Stat. Phys. Plasmas Fluids Relat. Interdiscip. Topics* **50,** 1579–1588 Medline
102. Weingarten, M. D., Suter, M. M., Littman, D. R., and Kirschner, M. W. (1974) Properties of the depolymerization products of microtubules from mammalian brain. *Biochemistry* **13,** 5529–5537 CrossRef Medline
103. Kirschner, M. W., Williams, R. C., Weingarten, M., and Gerhart, J. C. (1974) Microtubules from mammalian brain: some properties of their depolymerization products and a proposed mechanism of assembly and disassembly. *Proc. Natl. Acad. Sci. U.S.A.* **71,** 1159–1163 CrossRef Medline
104. Sandoval, I. V., and Vandekerckhove, J. S. (1981) A comparative study of the *in vitro* polymerization of tubulin in the presence of the microtubule-associated proteins MAP2 and tau. *J. Biol. Chem.* **256,** 8795–8800 Medline
105. Arnal, I., Karsenti, E., and Hyman, A. A. (2000) Structural transitions at microtubule ends correlate with their dynamic properties in *Xenopus* egg extracts. *J. Cell Biol.* **149,** 767–774 CrossRef Medline
106. Höög, J. L., Huisman, S. M., Sebo-Lemke, Z., Sandblad, L., McIntosh, J. R., Antony, C., and Brunner, D. (2011) Electron tomography reveals a flared

morphology on growing microtubule ends. *J. Cell Sci.* **124,** 693–698 CrossRef Medline

107. Wang, H. W., and Nogales, E. (2005) Nucleotide-dependent bending flexibility of tubulin regulates microtubule assembly. *Nature* **435,** 911–915 CrossRef Medline
108. Vitre, B., Coquelle, F. M., Heichette, C., Garnier, C., Chrétien, D., and Arnal, I. (2008) EB1 regulates microtubule dynamics and tubulin sheet closure *in vitro*. *Nat. Cell Biol.* **10,** 415–421 CrossRef Medline
109. Maurer, S. P., Cade, N. I., Bohner, G., Gustafsson, N., Boutant, E., and Surrey, T. (2014) EB1 accelerates two conformational transitions important for microtubule maturation and dynamics. *Curr. Biol.* **24,** 372–384 CrossRef Medline
110. Maurer, S. P., Bieling, P., Cope, J., Hoenger, A., and Surrey, T. (2011) GTPγS microtubules mimic the growing microtubule end structure recognized by end-binding proteins (EBs). *Proc. Natl. Acad. Sci. U.S.A.* **108,** 3988–3993 CrossRef Medline
111. Maurer, S. P., Fourniol, F. J., Bohner, G., Moores, C. A., and Surrey, T. (2012) EBs recognize a nucleotide-dependent structural cap at growing microtubule ends. *Cell* **149,** 371–382 CrossRef Medline
112. Devred, F., Barbier, P., Douillard, S., Monasterio, O., Andreu, J. M., and Peyrot, V. (2004) Tau induces ring and microtubule formation from αβ-tubulin dimers under nonassembly conditions. *Biochemistry* **43,** 10520–10531 CrossRef Medline
113. Lee, G., Cowan, N., and Kirschner, M. (1988) The primary structure and heterogeneity of tau protein from mouse brain. *Science* **239,** 285–288 CrossRef Medline
114. Goode, B. L., and Feinstein, S. C. (1994) Identification of a novel microtubule binding and assembly domain in the developmentally regulated inter-repeat region of tau. *J. Cell Biol.* **124,** 769–782 CrossRef Medline
115. Butner, K. A., and Kirschner, M. W. (1991) Tau protein binds to microtubules through a flexible array of distributed weak sites. *J. Cell Biol.* **115,** 717–730 CrossRef Medline
116. Lee, G., Neve, R. L., and Kosik, K. S. (1989) The microtubule binding domain of tau protein. *Neuron* **2,** 1615–1624 CrossRef Medline
117. Best, R. L., Chung, P. J., Benbow, S. J., Savage, A., LaPointe, N. E., Safinya, C. R., and Feinstein, S. C. (2017) Expression and isolation of recombinant tau. *Methods Cell Biol.* **141,** 3–26 CrossRef Medline
118. Miller, H. P., and Wilson, L. (2010) Preparation of microtubule protein and purified tubulin from bovine brain by cycles of assembly and disassembly and phosphocellulose chromatography. *Methods Cell Biol.* **95,** 3–15 CrossRef Medline